DYNAMIC SPECTRUM SCHEDULING AND MANAGEMENT IN CENTRALIZED COGNITIVE RADIO NETWORKS

by

Omar Khalid Sweileh

A Thesis Presented to the Faculty of the
American University of Sharjah
College of Engineering
in Partial Fulfillment
of the Requirements
for the Degree of

Master of Science in
Electrical Engineering

Sharjah, United Arab Emirates

November 2017

Approval Signatures

We, the undersigned, approve the Master's Thesis of Omar Khalid Sweileh

Thesis Title: Dynamic Spectrum Scheduling and Management in Centralized Cognitive Radio Networks.

Signature	**Date of Signature** (dd/mm/yyyy)
_____	_____
Dr. Mohamed Hassan Professor, Department of Electrical Engineering Thesis Advisor	
_____	_____
Dr. Hasan Mir Associate Professor, Department of Electrical Engineering Thesis Co-Advisor	
_____	_____
Dr. Mahmoud H. Ismail Associate Professor, Department of Electrical Engineering Thesis Committee Member	
_____	_____
Dr. Taha Landolsi Professor, Department of Computer Engineering Thesis Committee Member	
_____	_____
Dr. Nasser Qaddoumi Head, Department of Electrical Engineering	
_____	_____
Dr. Ghaleb Husseini Associate Dean for Graduate Affairs and Research College of Engineering	
_____	_____
Dr. Richard Schoephoerster Dean, College of Engineering	
_____	_____
Dr. Mohamed El-Tarhuni Vice Provost for Graduate Studies	

Acknowledgements

First, I would like to seize this opportunity to express my sincere gratitude to my advisors Prof. Mohamed Hassan and Prof. Hasan Mir for their continuous support to me throughout my Masters' thesis and research, for their patience, motivation, and enthusiasm. They always steered me in the right the direction whenever they thought I needed it. Their guidance helped me and I could've not imagined having a better advisors and mentors for my Masters' study.

Besides my advisors, I would also like to thank the rest of my thesis committee: Prof. Mahmoud Ismail, and Prof. Taha Landolsi, for their encouragement, and insightful comments. I would like to take this opportunity to also thank American University of Sharjah for rewarding me a Graduate Teaching Assistantship.

Last but not the least, I would like to thank my family: my parents Khalid Sweileh and Randa Issa, my sister Alaa', and my brothers Abdullah and Mohammad for their continuous support to me throughout my life.

Dedication

To my parent, brothers, and sister . . .

Abstract

As the demand for wireless radio spectrum increases, spectrum regulatory authorities expect to face a spectrum scarcity problem. Dynamic Spectrum Access (DSA) was recently proposed to enable efficient utilization of the radio spectrum. Cognitive Radio (CR)s are used to help in the realization of efficient DSA techniques. An integral component in Cognitive Radio Network (CRN), and in DSA in general, is scheduling, which has to do with the Secondary User (SU)'s ability to decide on the available spectrum that best meets its Quality of Service (QoS) requirements. Switching delay, which is defined as the time needed by a SU to hop among available channels, is a major factor that affects the performance of CRNs. This study is motivated by the fact that the literature is in need for efficient schedulers that can maximize the CRN's throughput while maintaining a minimum spectrum switching delay for the SUs. Specifically, two scheduling techniques are introduced with the aim of minimizing the switching delay and hence maximizing the amount of transmitted information over the underlying CRN. The first scheduler is an opportunistic spectrum and switching-delay aware scheduler with the objective of maximizing the total number of transmitted packets over the span of multiple time-slots. From the simulation results, the opportunistic scheduler, in highly dynamic channels, was able to transmit up to 20% more packets compared to the benchmark scheduling algorithm where the scheduling problem is done every time-slot. Moreover, the scheduler was able to reduce the effect of both switching and scheduling delays. On the other hand, the second proposed scheduler maximizes spectrum exploitation by allowing unscheduled SUs to utilize any idle spectrum during the switching delay. From the results, the proposed scheduler allowed for $\approx 38\%$ more SUs to be scheduled in an overpopulated CRN. Moreover, by utilizing the switching delay, the proposed scheduler was able to deliver around 4.5% more packets compared to the benchmark algorithm without sacrificing any complexity. In conclusion, both of the implemented schedulers delivered a higher amount of transmitted packets compared to the benchmark scheduling algorithms and both schedulers were able to reduce the effect of switching delay.

Search Terms: ***Dynamic spectrum access, cognitive radio networks*.**

Table of Contents

List of Figures

List of Tables

List of Abbreviations

AMC	Adaptive Modulation and Coding
ARQ	Automatic Repeat reQuest
BS	Base Station
CCCC	Common Control Communication Channel
CR	Cognitive Radio
CRN	Cognitive Radio Network
CS	Central Scheduler
CSA	Concurrent Spectrum Access
CSI	Channel State Information
DSA	Dynamic Spectrum Access
DT-FSMC	Discrete-Time Finite State Markov Chain
DT-MC	Discrete-Time Markov Chain
FCC	Federal Communications Commission
FSA	Fixed Spectrum Access
FSMC	Finite State Markov Chain
IoT	Internet of Things
LCR	Level Crossing Rate
MAC	Media Access Control
MC	Markov Chain
OSA	Opportunistic Spectrum Access
PER	Packet Error Rate

PHY	Physical Layer
PMF	Probability Mass Function
PU	Primary User
QoS	Quality of Service
SDR	Software Defined Radio
SNR	Signal to Noise Ratio
SU	Secondary User
UDP	User Datagram Protocol
VoIP	Voice over Internet Protocol
WSN	Wireless Sensor Network

Glossary

Fading channel is a wireless channel with a different sources of attenuation.

Internet of Things is a network of smart devices and sensors connected through the internet to enable them to communicate and interact among themselves.

Media access control is a sub-layer in data link layer that provides flow control and multiplexing for the physical communication link.

Signal to noise ratio is a measurement in engineering defined as ratio of signal power to background noise power.

Software defined radio is a communication radio system with software implemented components.

Telecommunications regulatory authorities are authorities responsible of regulating the use of wireless radio spectrum to improve spectrum usage.

Voice over internet protocol is a type of audio multimedia communications or voice communications over the internet.

Wireless sensor network is a wireless network of self-governing sensors and devices used to monitor physical and environmental condition in remote and diverse locations.

Chapter 1: Introduction

1.1. Significance of the Research

Over the last few years, the number of wireless devices and users have increased a multi-fold. As a result, spectrum regulators and telecommunications regulatory authorities expect to face difficulties in meeting such a growing demand. Studies forecast that the number of mobile subscribers will increase by almost one billion in 2020 compared to 2015 [1]. In addition to mobile users and with the growing attention on the concept of the Internet of Things (IoT), devices are also being wirelessly connected, thus imposing even more demand on the radio spectrum. A Gartner report predicts that the number of connected devices will reach almost 20 billion in 2020 [2]. One of the main challenges that we are currently facing is the limited radio spectrum [3]. Traditionally, telecommunications regulatory authorities were assigning a certain bandwidth to subscribers, where only licensed subscribers have the right to access that band or channel whenever required. On the other hand, unlicensed users are not allowed to utilize the spectrum, even if the licensed users are not using it. This policy is called Fixed Spectrum Access (FSA). As the number of wireless users increased in the last few years, the radio spectrum cannot physically cope with requirements of each application. As a result, this eventually led to a spectrum scarcity. In order to handle this increasing demand, a new policy called Dynamic Spectrum Access (DSA) was proposed [4]. DSA introduced the idea of allowing unlicensed users to utilize licensed spectrum without causing any interference to its licensed users. Studies and experiments, [5–7], have shown that the licensed users, or Primary User (PU) as referred to in the literature, are infrequently exploiting their spectrum in certain applications. This led to the idea of allowing unlicensed users, also known as Secondary User (SU), to utilize the licensed spectrum without causing any harm to the PUs. One way to do so is by allowing the SUs to opportunistically use the licensed spectrum whenever the PU is not using it. This is called Opportunistic Spectrum Access (OSA) and it's also known as interweave paradigm. Moreover, SUs are also allowed to share the spectrum with the PUs, if SUs will not cause any interference to the PUs. This is known as Concurrent Spectrum Ac-

cess (CSA) or spectrum underlay. In order to achieve that, the SUs' radios should have cognitive capabilities such as: learning and analyzing the spectrum and making spectrum decisions to maximize spectrum utilization. Such radios are known as Cognitive Radio (CR).

1.2. Background

The concept of CR was first proposed by Mitola in [4] as a part of software defined radio (SDR) to break some of the main limitations in wireless communications such as: inefficient spectrum utilization. Unlike traditional radio communication systems, SDRs can adapt to different changes in radio environment by varying their operating channel, modulation and coding schemes. CR was first proposed as an inclusive part of SDR, yet with time, it evolved and CR is currently in the core of any spectrum exploitation techniques in wireless communications. According to FCC [8], CR is defined as: "an intelligent wireless communication system capable of changing its transceiver parameters based on interaction with the external environment in which it operates," which makes it the main research topic in enabling spectrum utilization. The keys to do so are: spectrum awareness and sensing as well as dynamic spectrum scheduling and management. Spectrum awareness and sensing is a very crucial task in the interaction between CR and radio environment. Through spectrum awareness and sensing techniques, CRN should be aware of PUs status and activities. The level of awareness in any CR varies from the knowledge of PU activity to estimating PU signal to noise ratio (SNR) to even estimating the PU waveform [9]. After estimating the PU or spectrum status, the SUs should be able to select the most suitable channel to support their QoS requirements, then manage and coordinate the access to available spectrum among themselves. This is called dynamic spectrum scheduling and management.

CR is a smart entity by itself, yet, by allowing CRs to interact and by mobilizing their knowledge, an intelligent organization can be created. Such organization can help to enhance the overall spectrum exploitation. A group of CRs forms a Cognitive Radio Network (CRN) and CRNs, similar to any wireless networks, are classified as either centralized or decentralized networks as shown in Figure 1.1. Centralized net-

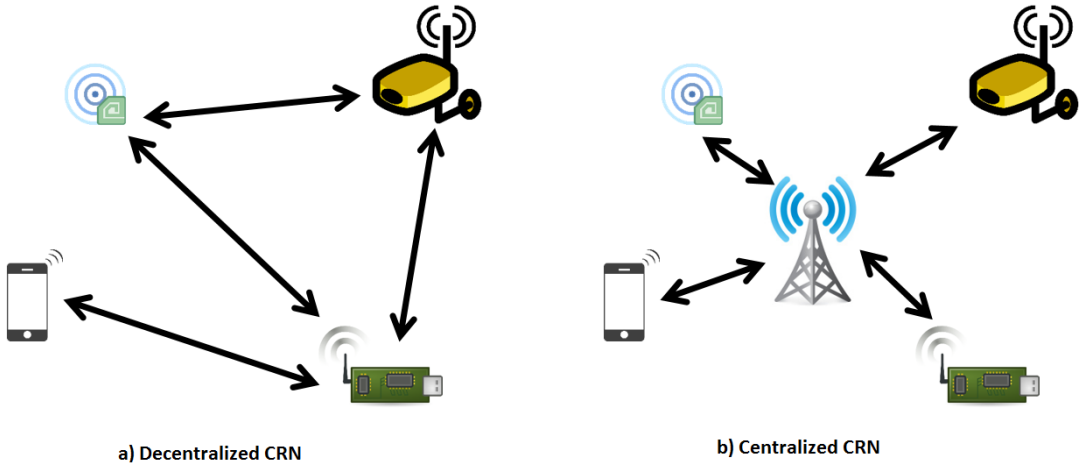

Figure 1.1: CRN architectures: (a) decentralized CRN, and (b) centralized CRN.

works, also known as infrastructure-based CRNs, have one focused centralized control point, which can be a Base Station (BS), that provides a single-hop communication to all of the CRN nodes. This centralized control node is usually referred to as spectrum server and primarily maintain control in the network. Since this central control point receives information from all nodes, then it has a global view of the whole network. This helps the centralized control point to make optimum decisions in terms of maximizing network throughput, spectrum fairness, efficiency, and priorities. However, this type of networks is difficult to integrate into current existing wireless networks due to its infrastructural nature. Unlike centralized CRNs, decentralized CRNs, also known as distributed or ad-hoc networks, do not have any centralized control point and network control is distributed among its nodes. Decentralized or Ad-hoc CRN uses peer-to-peer connections among its nodes. Due to the lack of centralized control point, the communication among network nodes require a route selection, which make this type of network architecture even more challenging than centralized one. Another big challenge in such networks is the synchronization among CRN nodes. This impose a great challenge, especially for synchronizing sensing periods in distributed CRNs. In order to sense the presence of PU in the spectrum, all SUs must stop their communications. Otherwise, SUs can cause corruption to the sensing process and CRN cannot tell whether a PU or a SU is using the spectrum. Such period, when all SUs halt their connections in order to sense the spectrum, is known as quiet period. In centralized CRNs, the BS can decide

the length of quiet period and synchronize it among all its nodes. Yet, in distributed CRNs, synchronizing the quiet period among network nodes is a very challenging task. Nonetheless, due to its infrastructure-less nature, decentralized CRNs have a great flexibility and thus are more easier to integrate into current deployed networks.

1.3. Problem Statement

CRNs have also introduced even more challenges to the concept of CR. Beside the challenges in cooperative spectrum sensing, one of the main challenges in CRNs is to schedule the access of SUs to the spectrum based on certain objective. Some of the main scheduling objectives discussed in literature are: maximizing the throughput of CRN, increasing the spectral utilization, reducing the interference to other PUs and SUs, ensuring fairness among CRN nodes, maintaining QoS requirement of different SUs traffic types, minimizing end-to-end delay, and, in some application, minimizing the SUs energy consumption. The scheduling process starts after the sensing process. The information from the spectrum sensing is worthless if it was not received correctly, analyzed intelligently, and employed wisely. Hence, making the dynamic spectrum scheduling and management a very critical and decisive task in CRNs. Dynamic spectrum scheduling and management is composed of three main keys: spectrum decision, spectrum sharing, and spectrum reallocation. Spectrum decision represents the scheduler ability to select the available band or channel that best suits SU's QoS requirement. Spectrum sharing, on the other hand, represents the collaboration among the SUs to access the available resources. Finally, spectrum reallocation is the SU's ability to leave the licensed spectrum whenever a PU is detected. Spectrum reallocation comes with the cost of less available transmission time. This occurs because, if the SU was assigned a new channel, then it will take some time to switch and adjust its transceiver electronics and hardware to operate on the new scheduled channel. Thus, resulting in a bandwidth loss. As a result, switching delay is a very crucial factor in the design of SU electronics [10]. Shorter spectrum switching delay will result in a larger, heavier, and more costly SU's equipment, which is inefficient. This happens due to the fact that fast spectrum switching time requires a larger number of filters [10], hence resulting in

heavier, larger and more expensive SU's hardware. As a result, switching delay is a very important factor in dynamic spectrum scheduling. Spectrum reallocation and spectrum decision problems are mainly studied separately in literature, which make investigating both subjects jointly an open research topic [11]. Consequently, the aim of this thesis is to create a scheduler that addresses both issues jointly. In other words, a major task of schedulers introduced in this thesis is to maximize the total number of transmitted packets over the underlying CRN while reducing the switching delay.

Chapter 2: Literature Review

Many dynamic spectrum scheduling techniques in centralized CRNs were proposed to address various scheduling objectives and challenges. When it comes to dynamic spectrum scheduling, few objectives are taken into consideration. One of the main objectives is to increase the CRN throughput or to increase the amount of successfully transmitted information in the CRN. Furthermore, since SU applications vary, their traffic is heterogeneous too and the CRN scheduler should take this into consideration while scheduling. Hence, another important objective is QoS requirements of each SU. Additionally, energy consumption of SUs should also be taken into account, especially for energy limited applications, like sensors in wireless sensor network (WSN). Moreover, the scheduler should also be capable of dealing with the arrival of PUs. Recall, the PUs have the highest priority and the scheduler must command the SUs that are using PU's spectrum to evacuate it once the PU arrives. As a result, the scheduler must also reallocate the displaced SUs to other available spectrum channels. This is known as spectrum reallocation or handoff. Table 2.1, below illustrates a general comparison among some dynamic spectrum scheduling papers based on the aforementioned objectives. In [12], a cross-layer design for a dynamic spectrum scheduling technique that takes into account the SU's session length was proposed. Liang *et al.* in [13] proposed a resource allocation and scheduling scheme for a relay CRN that maximizes the throughput and ensures a long-term fairness among SUs. Whereas in [14], the authors classified SUs traffic based on their application and focused more on spectrum reallocation of evacuated SUs. Furthermore, in [15, 16], scheduling schemes were proposed to maximize the throughput of the CRN while minimizing the energy consumption of SUs. The authors of [17–21] proposed scheduling schemes that ensure QoS satisfaction for different types of SU traffic, where [18] and [19] enforced admission control into SUs to check their eligibility to utilize spectrum and [20] adopted the idea of reserving available channels for future reallocation. In [22], Kannappa *et al.* proposed a dynamic service rate allocation for SUs to balance the network buffer and to reduce the buffers dropping probabilities, especially for real-time users or time sensitive applications. A relay based CRN that improves the CRN throughput by allow-

Table 2.1: General comparison between dynamic spectrum scheduling schemes based on their scheduling objective.

Reference	Throughput	Energy Efficiency	QoS	Spectrum Reallocation
[12]	✓		✓	
[13]	✓			
[14]				✓
[15]	✓	✓		
[16]	✓	✓		
[17]	✓		✓	
[18]			✓	✓
[19]			✓	✓
[20]			✓	✓
[21]			✓	✓
[22]	✓			
[23]	✓			
[24]	✓	✓	✓	
[25]	✓	✓		
[26]			✓	✓
[27]			✓	✓
[28]	✓			
[29]	✓			✓
[30]			✓	✓
[31]			✓	✓
[32]				✓
[33]				✓

ing cooperation among PUs and SUs was proposed in [23]. Furthermore, the authors in [24] and [25] proposed scheduling mechanisms that maximize the throughput and reduce energy consumption of SUs. Yet, the authors in [24] developed a more application specific scheduler that focuses on time-sensitive SUs such as video streaming SUs, and the authors of [25] proposed a joint spectrum sensing and spectrum scheduling optimization. In [26–28], the authors focused on spectrum reallocation (handoff) in CRN with heterogeneous SU traffic. Additionally, the authers in [29] focused on dynamic spectrum scheduling in CRN with Voice over Internet Protocol (VoIP) SUs where a two-tier CRN that utilizes talkspurt and silent suppression of VoIP traffic was proposed. On the other hand, the work in [30–33] aimed to reduce spectrum reallocation and such task in accomplished by modeling spectrum reallocation probabilistically based on PU's behavior. Furthermore, the contributions on this topic are not limited to

proposing scheduling and management schemes for CRN. For example, the authors of [34] built an analytical framework to analyze CRN throughput by modeling CRN using queuing theory while taking into consideration sensing errors, and link adaptation techniques like ARQ. Additionally, alternative methods, like improving the PU network to enhance CRN throughput by making PU's network more SU friendly, was proposed in [35]. Moreover, the work in [36] also focused on admission control of SUs to reduce SU's dropping and blocking probabilities.

Chapter 3: System Model and Assumptions

The main goal of dynamic spectrum scheduling and management in OSA-based CRN is to help in efficiently utilizing the wireless radio spectrum by allowing SUs to access licensed spectrum whenever the PU is not using it. Every time a PU leaves its spectrum, it creates a spectrum hole as shown in Figure 3.1. In centralized CRNs, SUs can then exploit these spectrum holes with the aid of a centralized scheduler. Then, the central control point or central scheduler task is to opportunistically schedule and manage the access of SUs to the underutilized licensed channels. Before scheduling, the central scheduler should receive and analyze the spectrum current occupancy and SUs states. Additionally, the central scheduler should also have a prior information about channels history and current channel quality. Then, the task of central scheduler is to schedule the available resources to SUs based on a certain objective. The objective of schedulers developed in this thesis is to maximize the amount of transmitted information in CRN while reducing the effect of switching-delay. Moreover, the schedulers should also prevent the SUs from causing any interference to the PUs. As shown in Figure 3.1, if the PU is not using its channel, then it will create a spectrum hole. According to the OSA, the SUs should capitalize these opportunities by utilizing the spectrum during them. Yet, when a PU becomes active and starts to seek its channel, then all SUs using its channel must evacuate it. This is due to the fact that PUs have the

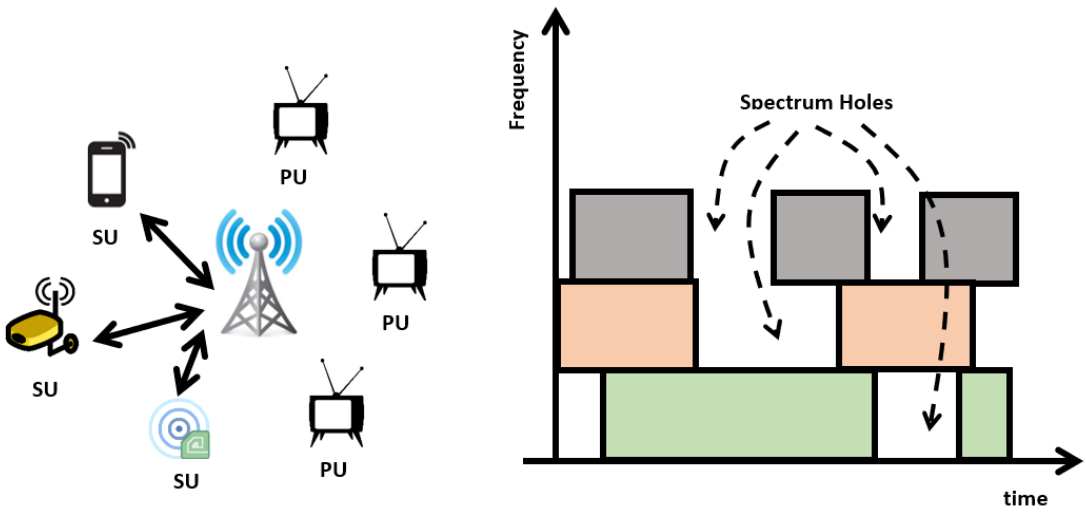

Figure 3.1: Illustration of spectrum holes and PUs spectrum exploitation over time.

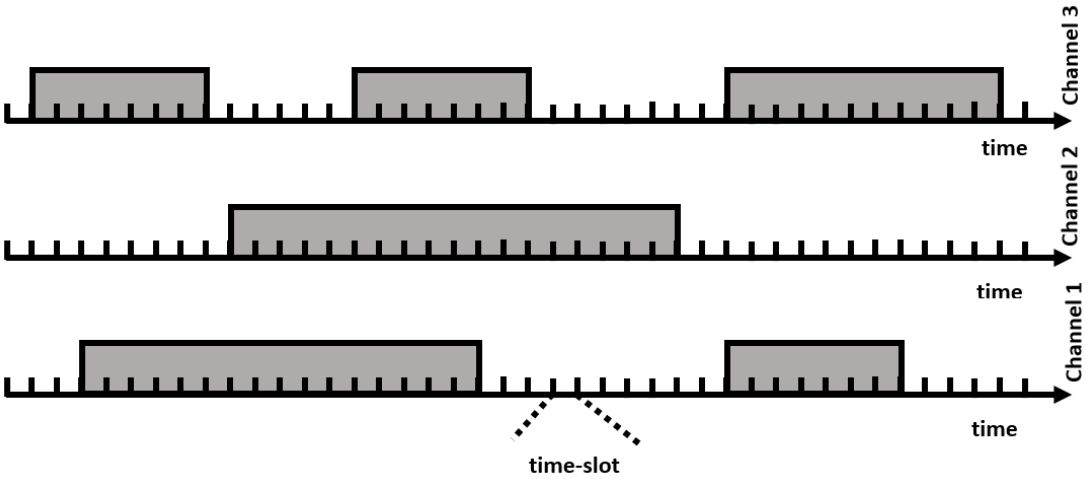

Figure 3.2: Discretization of time.

absolute priority over SUs, since they are the subscribers who paid to use the spectrum. An infrastructure-based network is considered in this thesis where a Central Scheduler (CS) is used as a control point for spectrum scheduling among CRN nodes. The thesis follows the OSA, hence the SUs are allowed to use the licensed spectrum only if the PU is not using it. Time is discretized in the simulations and the smallest time unit is called time-slot as shown in Figure 3.2. Additionally, the system parameters are assumed to be constant during time-slot and the parameters vary in a slot by slot basis.

3.1. Spectrum Model

Licensed spectrum is divided into a set of licensed bands or channels where $b_w \in \{b_1, b_2, ..., b_B\}$ represents licensed channel w. Each channel is composed of L sub-channels. Thus, the spectrum will have in total LB sub-channels as shown in Figure 3.3, where $l_j \in \{l_1, l_2, .., l_{LB}\}$ represents sub-channel j. Channels and sub-channels are dedicated for PUs and SUs, respectively. In other words, the PUs are entitled to use the whole channel while the SUs are allowed to use a single sub-channel for its connection [14]. This paradigm illustrates a more realistic model. For example, the PU can possibly represent a TV station where licensed spectrum consists of B-TV channels, and these TV channels are not being fully utilized. On the other hand, CRN can be thought of as a WSN, where this network is transmitting whenever the PUs are idle. Additionally, WSN sensors require smaller bandwidth compared to TV channels. The

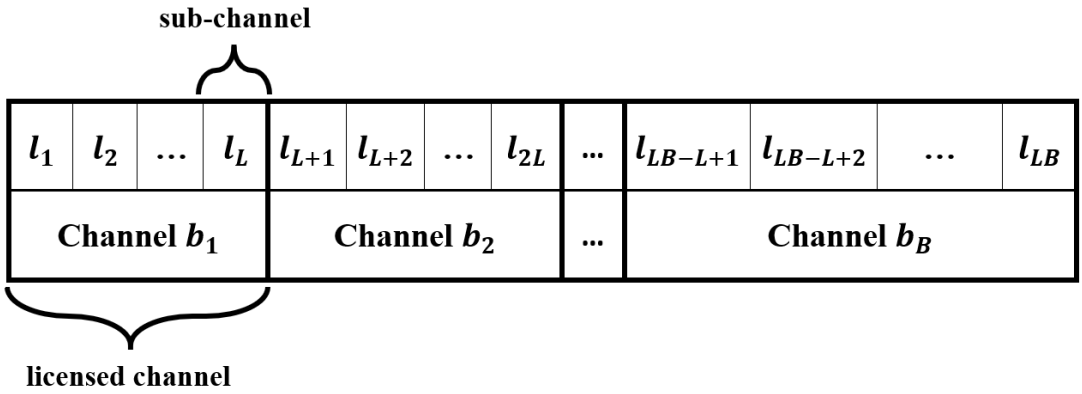

Figure 3.3: Licensed spectrum model.

traffic in the licensed channels vary from one channel to another. This heterogeneity can be classified using TV analogy, where TV channels have different activity rates. In addition to channels heterogeneity, the B channels are also assumed to be independent where channel's activity does not depend on the activities of other channels.

3.2. Primary Users and Secondary Users Model

Since channel availability is assumed to depend only on the PU activity, it is modeled in a way that is similar to the PU activity over the channel. In this thesis, each channel is assumed to be dedicated to a certain PU. The PU activity and SU activity are both modeled as a two-state Discrete-Time Markov Chain (DT-MC) with ON-and-OFF states, as illustrated in Figure 3.4. The model suggests that the ON-state indicates an active PU or SU, while the OFF-state indicates an idle PU or SU [33]. Moreover, as illustrated in Figure 3.4, the probability $p_{A,I}$ represents the transition probability from ON-state to OFF-state, and $p_{I,A}$ probability represents the transition probability from OFF-state to ON-state. The probability transition matrix of PU Markov Chain (MC) is:

$$P = \begin{bmatrix} p_{I,I} & p_{I,A} \\ p_{A,I} & p_{A,A} \end{bmatrix}. \tag{3.1}$$

where P represents transition probability matrix. Similar matrices are also used to model SU's MC. Since the PU traffic is also assumed to be heterogeneous, then each channel will have a different behavior compared to its neighbors. Additionally, the

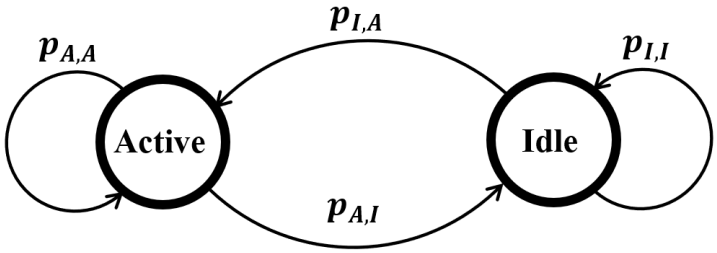

Figure 3.4: State transition diagram for PU/SU activity.

channels are assumed to be mutually independent where each channel will change its state independently from other channels. SUs activities are also assumed to be mutually independent. Two-state DT-MC representing the activity of PUs and SUs is composed of two recurrent states. Since this MC is a single irreducible class with aperiodic states, then it is a stationary MC. The stationary probabilities of both states are π_{active} and π_{idle}, and they are calculated as:

$$\pi_{active} = \frac{p_{A,I}}{p_{I,A} + p_{A,I}}, \tag{3.2}$$

$$\pi_{idle} = \frac{p_{I,A}}{p_{I,A} + p_{A,I}}. \tag{3.3}$$

The occupancy rate or activity rate of any channel or band is assumed to be known and such knowledge can be obtained from training and learning algorithms [37–39]. As mentioned earlier, time is discretized in these simulations and the smallest time unit is called time-slot. The system parameters are also assumed to be constant during any time-slot and the parameters vary in a slot-by-slot basis. For example, the PU activity or SU activity are assumed to be constant during any time-slot and their behavior changes in a slot-by-slot basis. The number of available sub-channels is denoted by χ_n where $0 \leq \chi_n \leq LB$ and number of busy sub-channel is $LB - \chi_n$. On the other hand, the number of SUs is denoted by S, and the number of active SU is denoted by S_n^{act} where $0 \leq S_n^{act} \leq S$. Note that, since the PUs and SUs activities are modeled as DT-MC, then they change over time and in slot-by-slot basis. Therefore, both χ_n and S_n^{act} are functions of time-slot n.

For the sake of illustrating the model, three PUs $B = 3$ are assumed to be licensed for three different channels. The PUs activity rates are assumed to be: 10%, 20%, and 30%. Based on these activity rates, three different probability transition ma-

Table 3.1: Simulated PU activity.

	PU activity	Simulated PU activity
PU #1	10%	9.96%
PU #2	20%	19.86%
PU #3	30%	29.85%

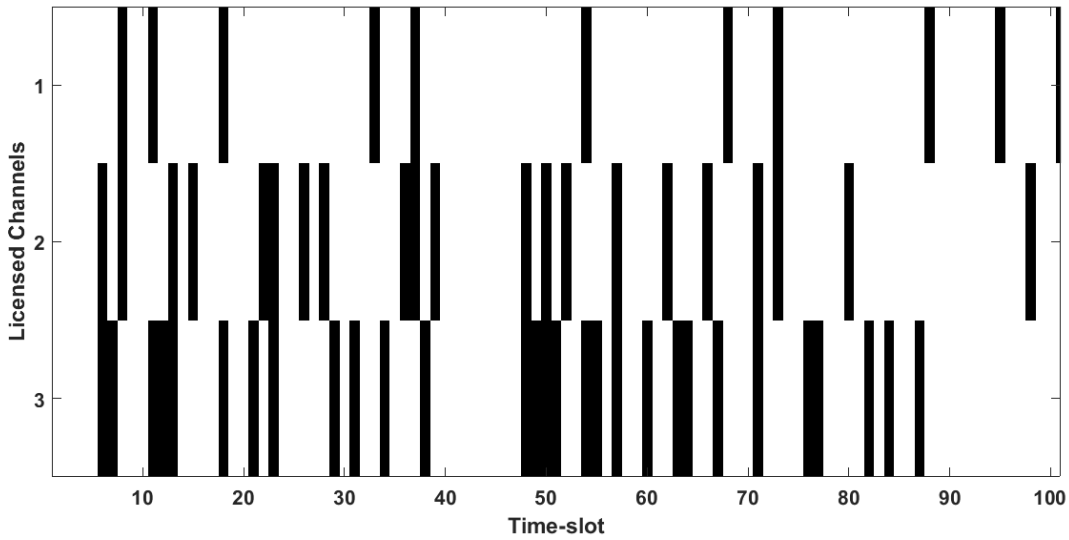

Figure 3.5: Licensed channels occupancy over 100 time-slots. (Black stripe represents a busy channel, and white stripe represents an idle channel)

trices are formulated accordingly. Table 3.1 shows the assumed PUs activity rates and the simulated PUs activity rates. In addition, Figure 3.5 illustrates the PUs activity rates or the channels occupancy over some time-slots. The white spaces represent the time-slots in which channels are idle or free to be used. Black stripes, on the other hand, represent the time-slots in which the licensed channels are busy and SUs are not allowed to use the channels. As seen from Figure 3.5, channel #3 has more black lines compared to the others and that's because it has a higher occupancy rate compared to the other two channels. On the contrary, channel #1 has the least black stripes because it has the lowest channel occupancy rate among the other channels.

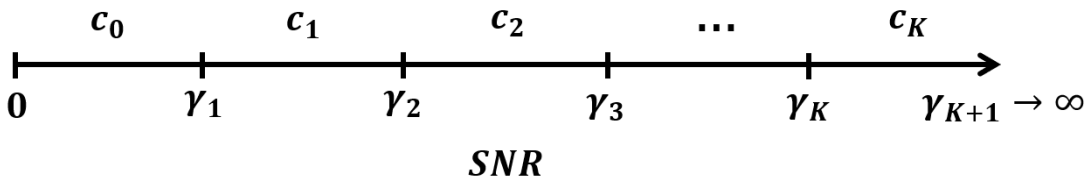

Figure 3.6: Partitioning the SNR range.

3.3. Channel Model

Each sub-channel is modeled as a Nakagami-m flat fading channel because Nakagami-m fading channel can represent a wide variety of fading channels. In this thesis, Channel State Information (CSI) is based on one parameter which is the received instantaneous signal to noise ratio (SNR) per packet. In order to find CSI, channel estimation techniques are used. Channel estimation process is always done at the receiver side. So, if an uplink system is assumed, where the receiver is a BS, then channel estimation is done by the BS. Otherwise, channel estimation is done by the SUs, then the CSI is sent back to BS through a Common Control Communication Channel (CCCC). In this thesis, an uplink system is assumed and channel estimation is done by the BS. Additionally, channel estimation is assumed to be perfect. The channel model, in this thesis, corresponds to a slow fading channel where the coherence time is larger than the time-slot. Moreover, the channel model also corresponds to a block fading channel model where instantaneous SNR is assumed to be fixed during predetermined time-slot and it varies in slot-by-slot basis [40]. Hence, the fading channel is modeled as a Discrete-Time Finite State Markov Chain (DT-FSMC), where the Finite State Markov Chain (FSMC) represents the variation of channel status over time. Consequently, Adaptive Modulation and Coding (AMC) is employed to improve the spectral efficiency of the CRN. In order to use AMC, the FSMC representing the channel needs to be first built. To build the FSMC representing channel, SNR range is partitioned. Based on a predetermined Packet Error Rate (PER), the whole SNR range is partitioned into a $K+1$ non-overlapping partitions as shown in Figure 3.6, where $K+1$ represents the number of the FSMC state representing the channel. Each partition represents an AMC mode c_k, where $1 \leq k \leq K$, except for the first partition c_0, which represents

Table 3.2: Transmission modes for uncoded square M-QAM modulation schemes.

	Mode #1	Mode #2	Mode #3	Mode #4	Mode #5
Modulation Scheme	BPSK	QPSK	8-QAM	16-QAM	32-QAM
c_k	1	2	3	4	5
a_k	67.7328	73.8279	58.7332	55.9137	50.0552
g_k	0.9819	0.4945	0.1641	0.0989	0.0381
γ_{pk}	6.3281	9.3945	13.9470	16.0938	20.1103

Table 3.3: Transmission modes of coded square M-QAM modulation schemes - Convolutional code.

	Mode #1	Mode #2	Mode #3	Mode #4	Mode #5
Modulation Scheme	BPSK	QPSK	8-QAM	16-QAM	32-QAM
c_k	$1/2$	1	$3/2$	3	$9/2$
Coding Rate	$1/2$	$1/2$	$3/4$	$3/4$	$3/4$
a_k	274.7229	90.2514	67.6181	53.3987	35.3508
g_k	7.9932	3.4998	1.6883	0.3756	0.0900
γ_{pk}	-1.5331	1.0942	3.9722	10.2488	15.9784

deep fade mode. During the deep fade mode, the transmitter is not allowed to transmit. The boundary points of partitions γ_k are determined based on the predetermined PER (PER_o). In order to partition the SNR range, PER expressions for each AMC mode need to be found. However, the PER expressions of the AMC modes are difficult to obtain, especially if coding is used. Thus, for the ease of calculation, PER functions used in finding the boundaries are an approximated PER expressions that are found by fitting PER function in Equation #3.4 to exact PER expressions of each transmission mode. The approximated PER expressions are given by [40]:

$$PER_k(\gamma) \approx \begin{cases} 1, & \text{if } 0 < \gamma < \gamma_{pk} \\ a_k \exp(-g_k \gamma), & \text{if } \gamma \geqslant \gamma_{pk} \end{cases}, \tag{3.4}$$

where a_k and g_k are fitting parameters and γ_{pk} is the start fitting PER point. The parameters a_k, g_k and γ_{pk} are functions of the AMC mode and they are calculated by fitting the approximated PER expressions to the exact PER curves. The AMC modes with their parameters are provided in Table 3.2 for uncoded adaptive modulation or Table 3.3 for adaptive modulation and coding using convolutional code [40]. In this thesis,

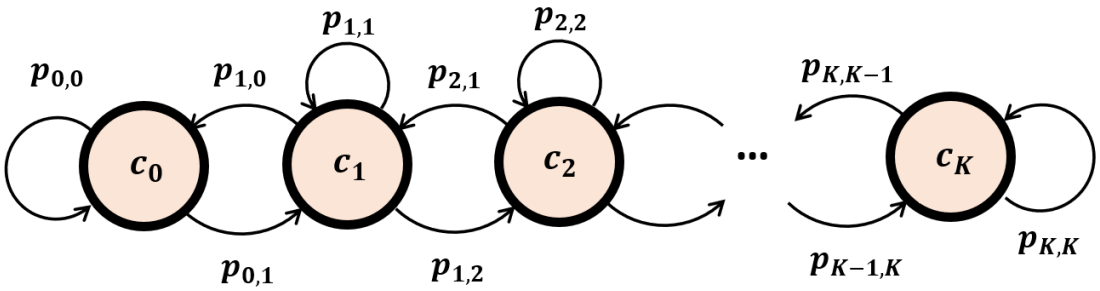

Figure 3.7: State transition diagram of Discrete-Time Finite State Markov Chain (DT-FSMC) channel model.

uncoded adaptive modulation is used. Accordingly, the boundaries of the AMC modes are obtained through solving the following equations [40]:

$$\gamma_0 = 0, \tag{3.5}$$

$$\gamma_k = \frac{1}{g_k} \ln\left(\frac{a_k}{PER_o}\right), \tag{3.6}$$

$$\gamma_{k+1} = +\infty, \tag{3.7}$$

and the AMC mode is determined based on which region does the instantaneous SNR lie:

$$c_k \in [\gamma_k, \gamma_{k+1}). \tag{3.8}$$

The AMC boundaries γ_k are found using a predetermined PER (PER_o). For the sake of demonstration, Figure 3.8 illustrates the boundaries of the SNR partitions for uncoded adaptive modulation. The boundaries were found using Equations #(3.5,3.6, and 3.7) and a predetermined PER $(PER_o = 0.001)$. The transition probability matrix of the channel FSMC is [41]:

$$P_c = \begin{bmatrix} P_{0,0} & P_{0,1} & 0 & \cdots & 0 & 0 & 0 \\ P_{1,0} & P_{1,1} & P_{1,2} & \cdots & 0 & 0 & 0 \\ 0 & P_{2,1} & P_{2,2} & \cdots & 0 & 0 & 0 \\ \vdots & \vdots & \vdots & \ddots & \vdots & \vdots & \vdots \\ 0 & 0 & 0 & \cdots & P_{N-1,N-2} & P_{N-1,N-1} & P_{N-1,N} \\ 0 & 0 & 0 & \cdots & 0 & P_{N,N-1} & P_{N,N} \end{bmatrix}, \tag{3.9}$$

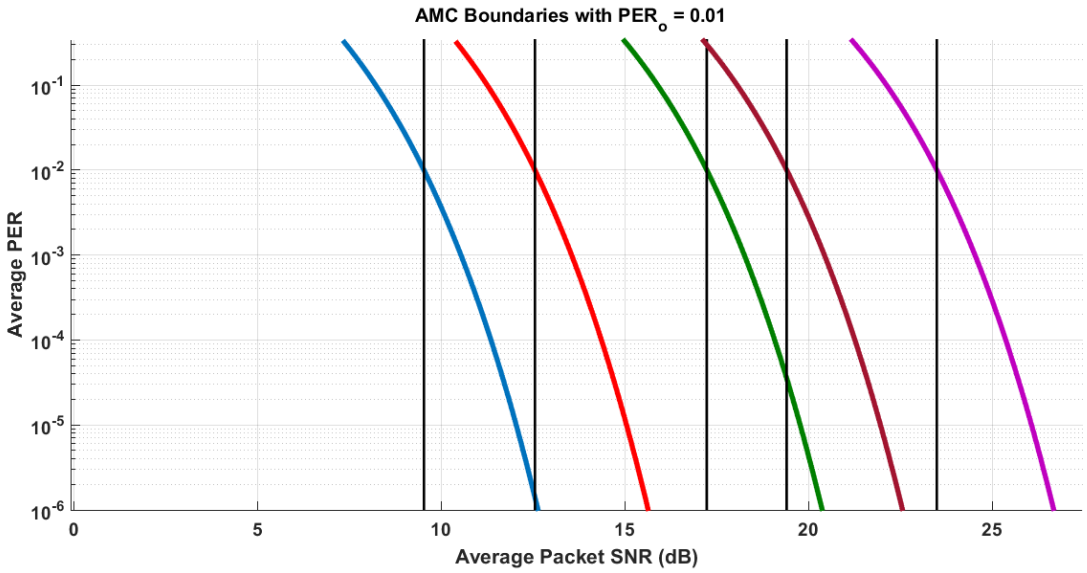

Figure 3.8: Boundaries of transmission modes for adaptive modulation without coding with $PER_o = 0.01$ and packet size of 1080 bits.

where $P_{a,b}$ represents the transition probability from CSI-a to CSI-b. As illustrated in Figure 3.7, the FSMC model representing the channel follows a birth-death model, and this can be seen from the tri-diagonal probability transition matrix where:

$$P_{a,b} = 0, \qquad |b-a| \geq 2. \tag{3.10}$$

The rest of the transition probabilities are calculated using average SNR $\bar{\gamma}$, Nakagami-m parameter m, and Doppler frequency f_d and they are found using [41]:

$$P_{k,k-1} = \frac{\eta_k T}{P_K(k)}, \tag{3.11}$$

$$P_{k,k+1} = \frac{\eta_{k+1} T}{P_K(k)}, \tag{3.12}$$

where T is the time-slot duration, $P_K(k)$ is the probability of c_k state to occur where c_k represents the AMC mode k, and η_k is Level Crossing Rate (LCR) of the channel in mode k. Probability of AMC mode k, $P_K(k)$, is found by:

$$P_K(k) = \int_{\gamma_k}^{\gamma_{k+1}} P_\gamma(\gamma) d\gamma = \frac{\Gamma(m, \frac{m\gamma_k}{\bar{\gamma}}) - \Gamma(m, \frac{m\gamma_{k+1}}{\bar{\gamma}})}{\Gamma(m)}, \tag{3.13}$$

where and $\Gamma(m) = \int_0^\infty \xi^{m-1} e^{-\xi} d\xi$ is the Gamma function and $\Gamma(m,x) = \int_x^\infty \xi^{m-1} e^{-\xi} d\xi$ is the upper or complementary incomplete Gamma function. Moreover, the LCR of Nakagami-m fading channel is found by [41]:

$$\eta_k = \sqrt{2\pi \frac{m\gamma_k}{\bar{\gamma}}} \frac{f_d}{\Gamma(m)} \left(\frac{m\gamma_k}{\bar{\gamma}}\right)^{k-1} \exp\left(\frac{m\gamma_k}{\bar{\gamma}}\right). \tag{3.14}$$

The rest of transition probabilities are calculated using the second axiom of probability and they are found using:

$$p_{k,k} = \begin{cases} 1 - p_{k,k+1} - p_{k,k-1}, & if \;\; 0 < k < K \\ 1 - p_{0,1}, & if \;\; k = 0 \\ 1 - p_{N,N-1}, & if \;\; k = K \end{cases}. \tag{3.15}$$

3.4. Assumptions

For the rest of the system and operation assumptions, each SU is assumed to have a unique ID. A CCCC is assumed for the communications between SUs and BS of CRN. The CCCC is assumed to be be an error-free narrowband channel with no latency. Additionally, in this thesis, the sub-channels are classified into three categories:

1. Protected sub-channels: which are sub-channels in an occupied channel.
2. Scheduled sub-channels: which are sub-channels occupied by SUs.
3. Candidate sub-channels: which are idle sub-channels that are not utilized by any SU.

Moreover, it is assumed that the underlying CRN employs a best effort User Datagram Protocol (UDP) where retransmissions are not allowed and thus incorrectly received packets are dropped. Furthermore, similar to cognitive radio standard IEEE 802.22, SUs are assumed to have one transceiver. Hence, each SU requires only one sub-channel to operate on [42]. Finally, a single sub-channel should only serve a single SU.

Chapter 4: Dynamic Spectrum Scheduling and Management

4.1. Media Access Control Framework

Unlike wireless networks, CRNs are required to operate in a changing spectrum and unsteady environment with limited resources. This led to modifications in its network protocols. For example, AMC is employed in the Physical Layer (PHY) in order to adapt to changing environment and to improve the spectral efficiency. Additionally, new Media Access Control (MAC) protocol is designed to mainly utilize the changing and limited spectrum. This section will go through the MAC protocol for centralized CRNs. Assuming that the communications between the BS and CRN nodes is synchronized, dynamic spectrum scheduling and management occur periodically every time-slot. Communications during time-slots are done using a MAC framework as shown in Figure 4.1. During each time-slot, three to four tasks are carried out depending on the scheduling result. First, the most important task is to sense the PU activity or channel occupancy. Depending on the type of the CRN, the sensing process is carried by either the SUs or the BS. In Ad-hoc networks, the SUs sense the spectrum. However, in centralized CRNs, the sensing process can be done by either the SUs or the BS. During the sensing period, all SUs must halt their communications in order to sense PUs in the spectrum. Otherwise, the interference from SUs' signals will cause a disturbance to the sensing process. Afterward, the control phase is carried out. In this phase, the SUs will send all their information and sensing results, if any, to the BS. Thereafter, the CS will start the scheduling process before broadcasting the scheduling results to the entire CRN nodes. If a SU was not assigned a sub-channel, then it will get in to the idle phase as illustrated in Figure 4.1(b). Otherwise, if required, the SU will first adjust its transceiver to operate on the new scheduled channel, then it will start transmitting as shown in Figure 4.1(a).

4.1.1. Spectrum Sensing. Spectrum sensing is one of the most crucial tasks in any CRN. Spectrum sensing was developed to help CR identify the spectrum status and to help create more opportunities for SUs. Additionally, accurate sensing is required because if a PU is detected, then the utilized spectrum bands have to be evacu-

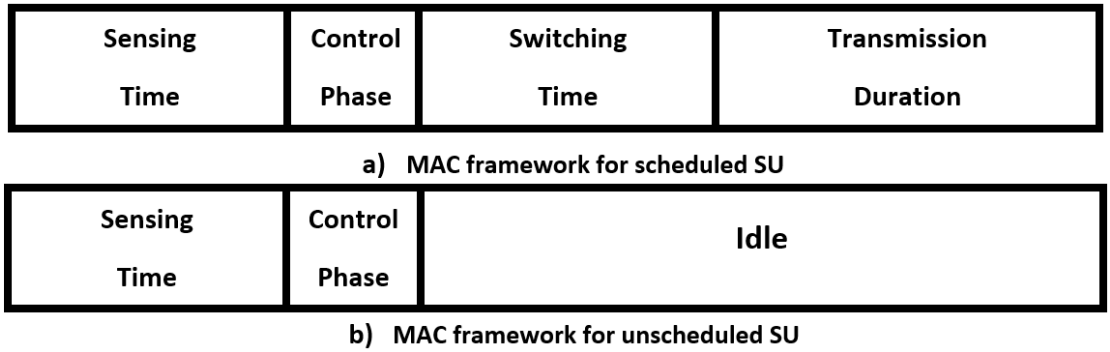

Figure 4.1: Structure of MAC framework for different scenarios: (a) MAC framework for scheduled SU and (b) MAC framework for unscheduled SU.

ated. Recently, multiple spectrum sensing techniques were developed such as: matched filter detection, energy detection, and feature detection [43]. In CR standards, such as IEEE 802.22, the spectrum sensing technique is not usually specified, and standards mainly allow for any spectrum sensing technique. However, even though the detection mechanism is not specified, standards usually specify certain conditions that CRN and its nodes must satisfy. Some of these conditions are maximum allowed time to sense and maximum time given for SU to leave the channel [44]. In this thesis, it is assumed that there is no interaction between the SUs and the PUs. Hence, SUs do not have any knowledge regarding the PU's transmission. Additionally, the sensing process is assumed to be perfect and the aim of this process is to detect whether the PU is active or not. The sensing time in this thesis is denoted by t^{sen}.

4.1.2. Control Phase. After the sensing phase is carried out, all the information required for the scheduling process must be sent to CS through CCCC. Every SU will send its unique ID, the operating frequency of its transceiver, and its status to the CS. As mentioned in Section #3.2, SU status is either ON or OFF, where the ON-state indicates an active SU and the OFF-state represents an idle SU. Afterward, given the sensing results, the SU status and the CSI, the CS in the BS will perform the scheduling algorithm based on certain objective function. In this thesis, the main objective function is to maximize the total number of transmitted packets from CRN while reducing the switching-delay effect. The details of scheduling algorithms are discussed later in Chapters #5 and #6. After the scheduling is performed, the BS will then broadcast

the scheduling results to all the SUs in the CRN. The broadcast will contain each sub-channel with SU assigned to it. Moreover, the broadcast will also contain the time set of each scheduled SU to start and stop their transmission. In this thesis, the control phase duration is denoted by t^c.

4.1.3. Switching and Transmission Phase. If the SU was not assigned a sub-channel, then it will not transmit and it will stay idle till the end of the time-slot. However, if the SU was assigned a sub-channel, then it will first switch its transceiver to operate on the new scheduled sub-channel. Afterward, it will start transmitting till the end of the time-slot. It is worth mentioning that the switching phase is not a mendatory phase because the CS can schedule the SU to its previous sub-channel. Thus, eliminating the need for the SU to adjust its transciever. In this section, the focus will be on the switching and transmission phases. In order to find the amount of transmitted information, the transmission time must be first found. To find the transmission time, the duration of the rest of framework phases must be defined and found. Note that, the sensing duration and control phase duration are fixed. Hence, after defining the sensing phase and the control phase, the switching phase is defined. Switching delay, in literature, is defined as the time required to find an idle sub-channel, or even the routing delay in distributed CRNs. However, in this thesis, switching delay is defined as the time required for the SU to adjust its transceiver's operating frequency to the new scheduled frequency. Shorter spectrum switching delay will result in a larger, heavier, and more costly SU equipment, which is inefficient. This is due to the fact that fast spectrum switching time requires more filters [10]. As a consequence, the switching delay plays an important role in the CR design process and it is a very crucial factor in the selection the CR electronics [10]. The delay associated with spectrum switching depends mainly on old and new sub-channels, and for simplicity, such relation is assumed to be linear and is found as follow [45]:

$$t_n^{sw} = v^{sw} \left| f_n^{new} - f_n^{old} \right|, \tag{4.1}$$

where f_n^{new} is frequency of new scheduled sub-channel, f_n^{old} is the frequency of old sub-channel, and v^{sw} is the switching latency factor which represents the time that requires

the SU to move in the spectrum and it's measured in seconds per unit bandwidth (Hz). The switching time is not constant and it varies in a slot-by-slot basis depending on the scheduling result. As a result, the switching delay is a function of time-slot n. After the switching is done, the SU can start the transmission till the end of the time-slot. After defining all the MAC framework phases, the transmission time is thus calculated as follows:

$$t_n^{tr} = \max\left(0, T - \left(t^{sen} + t^c + t_n^{sw}\right)\right), \tag{4.2}$$

where T is the time-slot duration. Theoretically, it is possible for the switching delay to be more than the available time where $t_n^{sw} > T - (t^{sen} + t^c)$. Such cases will result in a negative transmission time $t_n^{tr} < 0$. Therefore, the $\max(.)$ function is used to account for such cases.

4.2. Benchmark Scheduling Algorithm

After sensing the spectrum, based on the available and sensed information, the CS must distribute the available spectrum resources among the contending SUs. Managing and distributing the available resources to contending SUs is a scheduling problem as illustrated in Figure 4.2. As shown in Figure 4.2, after obtaining all the required information: PU activity, SU availability and CSI of each SU in each sub-channel, it is the CS job to schedule and distribute the available sub-channels to active SUs based on a certain objective function. The objective function can be, for example, to manage SUs access to the spectrum while maximizing the throughput of the secondary network or CRN, maximizing the spectral utilization, reducing the interference to other PUs and SUs, ensuring fairness among CRN nodes, maintaining QoS requirement for different SUs traffic types, reducing end-to-end delay and, in some application, minimizing the SUs energy consumption. The scheduling problem in this thesis evolves around maximizing the total amount of transmitted information in the CRN while reducing the effect of switching delay. Two scheduling algorithms are proposed in this thesis to encounter this issue. Before introducing these scheduling algorithms, a benchmark scheduling algorithm is introduced where this scheduling algorithm will be used as a benchmark reference point to help us study CRN performance of different scheduling algorithms.

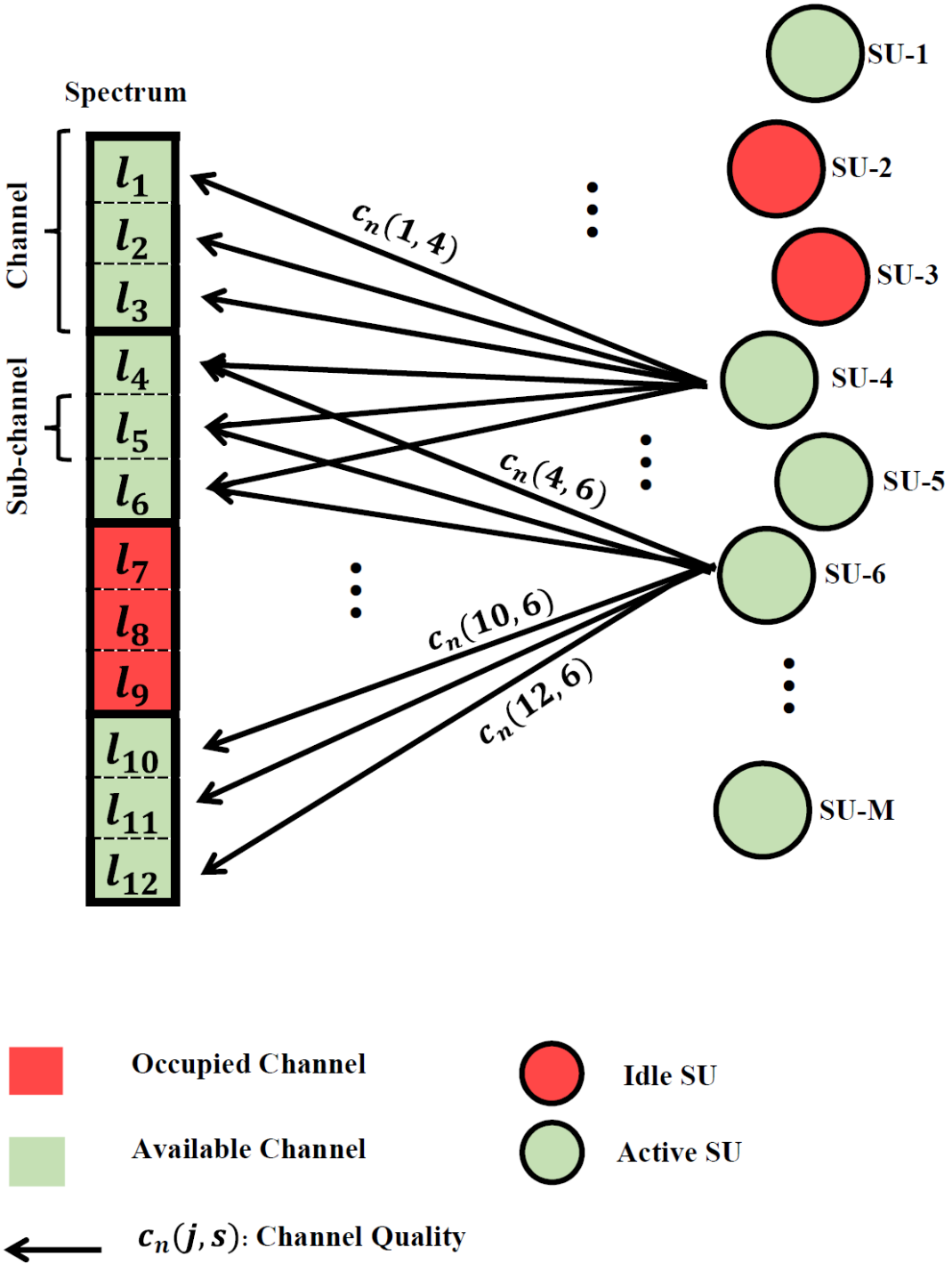

Figure 4.2: Illustration example of scheduling problem model of CRN where active SUs (right) need to be scheduled to available spectrum sub-channels (left) based on a certain objective function.

The benchmark scheduling algorithm main objective is to maximize the total number of transmitted packets in the CRN. The scheduling problem is performed every time-slot during the control or scheduling phase of the MAC framework. The aim now is to define the number of transmitted packets in terms of the transmission mode and the transmission duration. The number of transmitted packets that SU s can transmit on sub-channel j during time-slot n is calculated as follow:

$$R_n(j,s) = u_n(j)e_n(s)Y_n(j,s)t_n^{tr}(j,s), \tag{4.3}$$

where $u_n(j) \in \{0,1\}$ is the PU state in sub-channel j at time-slot n, $e_n(s) \in \{0,1\}$ is the SU state of user s at time-slot n, and $Y_n(j,s)$ represents the amount of packets that SU s can transmit on sub-channel j during time-slot n, and it's given by [41]:

$$Y_n(j,s) = \left(\frac{R_b}{L_p}\right) c_n(j,s), \tag{4.4}$$

where $c_n(j,s) \in \{0,1,...,K-1\}$ is the channel mode of user s on sub-channel j at time-slot n, R_b is the bit rate and L_p is the packet size. From the definition, it can be seen that the channel quality, the SU activity and the spectrum occupancy are accounted for in the definition using the indicator variables $c_n(j,s)$, $e_n(s)$ and $u_n(j)$, respectively. Hence, if the SU is not active, $e_n(s) = 0$, or if the channel is occupied, $u_n(j) = 0$, then the number of transmitted packets will be zero. Afterward, the CS needs to schedule SUs into the available spectrum. An optimization problem is formulated and it is a binary integer problem. The optimization problem is formulated as follows [45]:

$$\max_{\vec{X}} \quad \sum_{j=1}^{LB}\sum_{s=1}^{S} X(j,s)R_n(j,s), \tag{4.5}$$

$$\text{subject to} \quad X(j,s) \in \{0,1\}, \tag{4.6}$$

$$\sum_{j=1}^{LB} X(j,s) \leq 1, \quad s \in \{1,\cdots,S\}, \tag{4.7}$$

$$\sum_{s=1}^{S} X(j,s) \leq 1, \quad j \in \{1,\cdots,LB\}, \tag{4.8}$$

where variable $X(j,s)$ represents the binary decision variable of user s at sub-channel j and $\overrightarrow{x} = \left[X(j,s)\right]$ where $j \in \{1,\cdots,LB\}, s \in \{1,\cdots,S\}$ is the decision vector. The CS needs to also take into consideration some predetermined constraints. Constraint (4.6) indicates that the decision variable must be a binary variable, where $X(j,s) = 0$ indicates that SU s is not assigned to sub-channel j and $X(j,s) = 1$ indicates that SU s is assigned to sub-channel j. On the other hand, constraint (4.7) represents the fact that each CR has one transceiver and can only utilize one sub-channel. Similarly, constraint (4.8) prevents multiple simultaneous utilization of a single sub-channel. The optimization problem tries to solve and find $\overrightarrow{x}$ that provides the maximum number of transmitted packets given the above constraints.

Chapter 5: Opportunistic Scheduling Algorithm

The sensing process is fundamental and must be performed every time-slot to ensure the protection and the integrity of PU. Otherwise, the SUs can cause an undesired interference to PUs. On the other hand, scheduling is performed in order to distribute the spectrum resources among contending SUs. Furthermore, the switching-delay will always occur whenever the CS orders a SU to switch its current sub-channel. Hence, the switching delay occurs always after the scheduling phase as shown in Figure 5.1. Both scheduling and switching delays consumes bandwidth. Thus, the aim of the scheduling algorithm introduced in this chapter is to reduce the effect of both scheduling and switching delays. This is done by performing the scheduling process once every multiple time-slots as in Figure 5.1(b) instead of every time-slot as in Figure 5.1(a), hence reducing the waste in bandwidth caused by both delays. However, if a PU is idle during current time-slot, it might become active in the next time-slot, thus preventing the SU from transmitting. Alternatively, if a SU is active during current time-slot, it might become idle in the next time-slot, thus wasting a transmission opportunity. Therefore, scheduling a SU to a certain sub-channel over the span of multiple time-slots is a complicated task. Nonetheless, the scheduling algorithm should be able to deal with the changing and unsteady behavior of the CRN. Such task can be achieved by intelligently employing the PU, SU, and channel probabilistic models that were developed in Chapter #3. The idea behind this scheduling algorithm is to maximize the expected number of transmitted packets in the CRN over the span of multiple time-slots. The expected number of transmitted packets is obtained using an estimation algorithm. This scheduler is called an opportunistic scheduling algorithm.

The idea behind this scheduler is to increase the amount of transmitted information by allowing the SUs to switch their channels every multiple time-slots, hence reducing the time consuming effect of both switching and scheduling delays. This work was first proposed in [46]. However, the proposed scheduler is built to help decrease the effect of only the scheduling delay, and does not take switching delay into consideration. Since scheduling delay is fixed, it is easily accounted for in opportunistic scheduler. On the other hand, the delay associated with spectrum switching depends

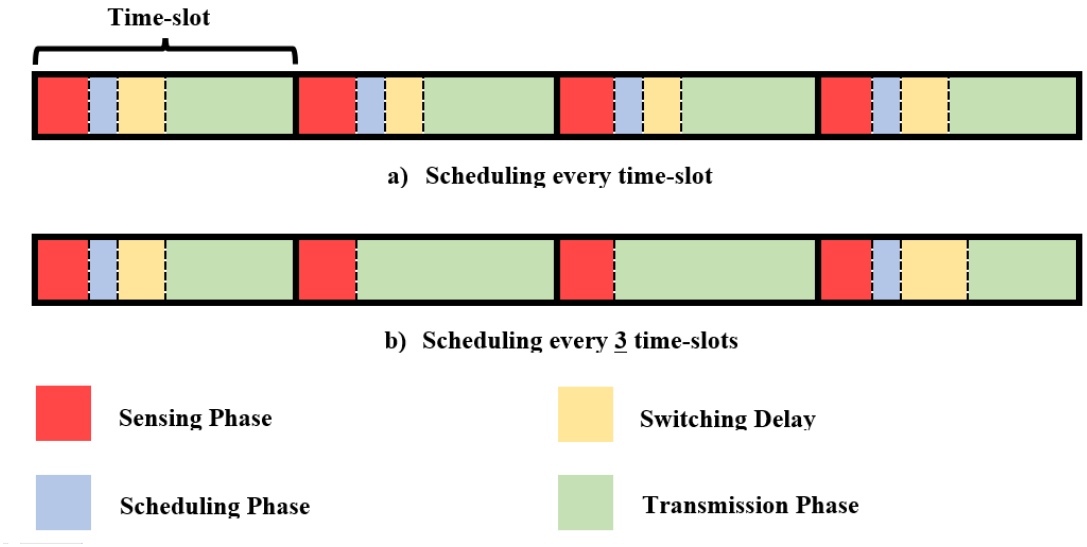

Figure 5.1: Scheduling routine for: (a) benchmark scheduling algorithm where scheduling occur every time-slot, and (b) opportunistic scheduling algorithm where scheduling occur every multiple time-slots.

mainly on current channels and new scheduled channels [10], which makes it, unlike the scheduling delay, a random delay. In addition of being random, the switching delay is also a function of channel bandwidth and it mainly depends on the SU's electronics. Moreover, the scheduler used in [46] uses a heuristic scheduling algorithm. In contrast, the scheduler used in this thesis employs an optimization algorithm to solve the scheduling problem. An optimization problem is formulated and solved to find the optimum solution.

5.1. Estimation Process

As mentioned before, the aim of this scheduler is to allow the SUs to switch their channels over the span of multiple time-slots, which will reduce the effect of the switching delay. Hence, the scheduling process will occur every N time-slots, where N is called the scheduling period. Based on the assumptions in Section #4.2 and as Figure 4.2 illustrates, at the beginning of every scheduling or control phase, the CS should know $u_n(j) \in \{0,1\}$, the PU state of sub-channel j at time-slot n, $e_n(s) \in \{0,1\}$, the SU state of user s at time-slot n, and $c_n(j,s) \in \{0,1,...,K-1\}$, and the channel mode of user s on sub-channel j at time-slot n. Then, the system is modeled as a multi-dimension MC based on the models discussed in Chapter #3. Each state is represented

by PU activity, SU status, and CSI, where the states of multi-dimensional MC is denoted by $\mathbf{y_n}(\mathbf{j},\mathbf{s}) = \big(u_n(j) = i, e_n(s) = m, c_n(j,s) = k\big)$ or for simplicity (i,m,k). The probability of state (i,m,k) to occur is represented by the joint Probability Mass Function (PMF) of state (i,m,k). The joint PMF of state (i,m,k) is denoted by $p_n\left(\mathbf{y_n}(\mathbf{j},\mathbf{s})\right) = p_n\left(u_n(j) = i, e_n(s) = m, c_n(j,s) = k\right)$ or for short $p_n(i,m,k)$. Additionally, the joint PMF state vector, denoted by Π_n, is a vector of size $(2 \times 2 \times (K+1))$ that contains the joint PMF probabilities of all states in multi-dimension MC. Note that, the state vector is also a function of time-slot n where $n \in \{1,...,N\}$. Since the system is modeled as MC, all the joint PMFs can be specified using the initial joint PMF and the probability transition matrix of MC. Initial joint PMF is found based on measured and shared information at the beginning of first time-slot. The PMF state vector of first time-slot is:

$$\Pi_1 = \begin{cases} 1, & i = i^*, m = m^*, k = k^* \\ 0, & otherwise \end{cases}, \tag{5.1}$$

where i^*, m^*, and k^* are the observed and sensed PU activity, SU state, and CSI at first time-slot, respectively. From the measurements and shared information, the CS can then find the number of transmitted packets of SU s at sub-channel j during first time-slot $n = 1$. Afterward, the joint probabilities of the rest of the time-slots are found using conditional PMFs and initial PMF:

$$\Pi_{n+1} = \mathbf{P}\Pi_n, \tag{5.2}$$

where $\mathbf{P}$ is the transition probability matrix of multi-dimension MC and is given by:

$$\mathbf{P} = \begin{bmatrix} p\left(0,0,0|0,0,0\right) & p\left(0,0,1|0,0,0\right) & \cdots & p\left(1,1,K|0,0,0\right) \\ p\left(0,1,0|0,0,1\right) & p\left(0,0,1|0,0,1\right) & \cdots & p\left(1,1,K|0,0,1\right) \\ \vdots & \vdots & \ddots & \vdots \\ p\left(0,0,0|1,1,K\right) & p\left(0,0,1|1,1,K\right) & \cdots & p\left(1,1,K|1,1,K\right) \end{bmatrix}, \tag{5.3}$$

$$\mathbf{P} = \Big[p\left(i',m',k'|i,m,k\right)\Big], \tag{5.4}$$

where $p\left(i',m',k'|i,m,k\right)$ is the transition probability from state $(u_n(j)=i, e_n(s)=m, c_n(j,s)=k)$ to state $\left(u_{n+1}(j)=i', e_{n+1}(s)=m', c_{n+1}(j,s)=k'\right)$. Hence, state $\left(i',m',k'\right)$ can be obtained using:

$$p_{n+1}\left(i',m',k'\right)=\sum_{i,m,k} p\left(i',m',k'|i,m,k\right) p_n\left(i,m,k\right). \tag{5.5}$$

The transition probabilities are found using Bayes' theorem where the transition conditional probability is [46]:

$$\begin{aligned} p\left(i',m',k'|i,m,k\right) &= \frac{p\left(i',m',k',i,m,k\right)}{p\left(i,m,k\right)} \\ &= p\left(i'|m',k',i,m,k\right)\frac{p\left(m',k',i,m,k\right)}{p\left(i,m,k\right)} \\ &= p\left(i'|m',k',i,m,k\right) p\left(m',k'|i,m,k\right). \end{aligned} \tag{5.6}$$

By continuing the derivation using the same steps as above, the transition probability is found to be:

$$p\left(i',m',k'|i,m,k\right)=p\left(i'|m',k',i,m,k\right) p\left(m'|i',k',i,m,k\right) p\left(k'|i',m',i,m,k\right). \tag{5.7}$$

As per the models in Chapter #3, the PU state only depends on the PU state of previous time-slot, and the SUs or the CSI do not play any rule in whether the PU should be transmitting or not. Additionally, channel mode only depends on previous channel mode and it is independent of both PUs activity and SUs activity. Moreover, the SU state depends only on the SU previous state. As a result, the transition conditional probability is:

$$p\left(i',m',k'|i,m,k\right)=p\left(i'|i\right) p\left(m'|m\right) p\left(k'|k\right), \tag{5.8}$$

where all the transition probabilities are from the models discussed in Chapter #3. Using the transition probabilities, the probability transition matrix, **P**, of multi-dimension MC is formulated. Thus, the PMF state vector of time slot $n+1$ can be found using the probability transition matrix and the PMF state vector of time-slot n via Equation #5.2. The scheduling of the SUs is based on the estimated number of transmitted packets of

each SU at each sub-channel during the span of N time-slots. Such expected value is found using the modeled multi-dimension MC. The estimated number of transmitted packets during N time-slots is simply the sum of the expected number of transmitted packets in every time-slot n during scheduling period N:

$$\widetilde{R}(j,s) = \sum_{n=1}^{N} \widetilde{R}_n(j,s), \tag{5.9}$$

where $\widetilde{R}_n(j,s)$ is the expected number of transmitted packets of SU s at sub-channel j during time-slot n and it is found as follow:

$$\widetilde{R}_n(j,s) = \sum_{i,m,k} p_n(i,m,k)\, R(i,m,k), \tag{5.10}$$

where $R(i,m,k)$ is the number of transmitted packets of state (i,m,k) in multi-dimension MC.

5.2. Scheduling Algorithm

Unlike the scheduler in [46], the scheduling process in this thesis is done using an optimization algorithm and not a greedy algorithm. Similar to the benchmark algorithm in Section #4.2, the scheduler main objective is to maximize the expected number of transmitted packets in the CRN. However, unlike the benchmark algorithm where scheduling is done every time-slot, the optimization problem in the opportunistic algorithm is formulated every N time-slots as follow:

$$\max_{\vec{x}} \quad \sum_{j=1}^{BL} \sum_{s=1}^{S} X(j,s)\widetilde{R}(j,s), \tag{5.11}$$

$$\text{subject to} \quad X(j,s) \in \{0,1\}, \tag{5.12}$$

$$\sum_{j=1}^{LB} X(j,s) \leq 1, \quad s \in \{1,\cdots,S\}, \tag{5.13}$$

$$\sum_{s=1}^{S} X(j,s) \leq 1, \quad j \in \{1,\cdots,LB\}, \tag{5.14}$$

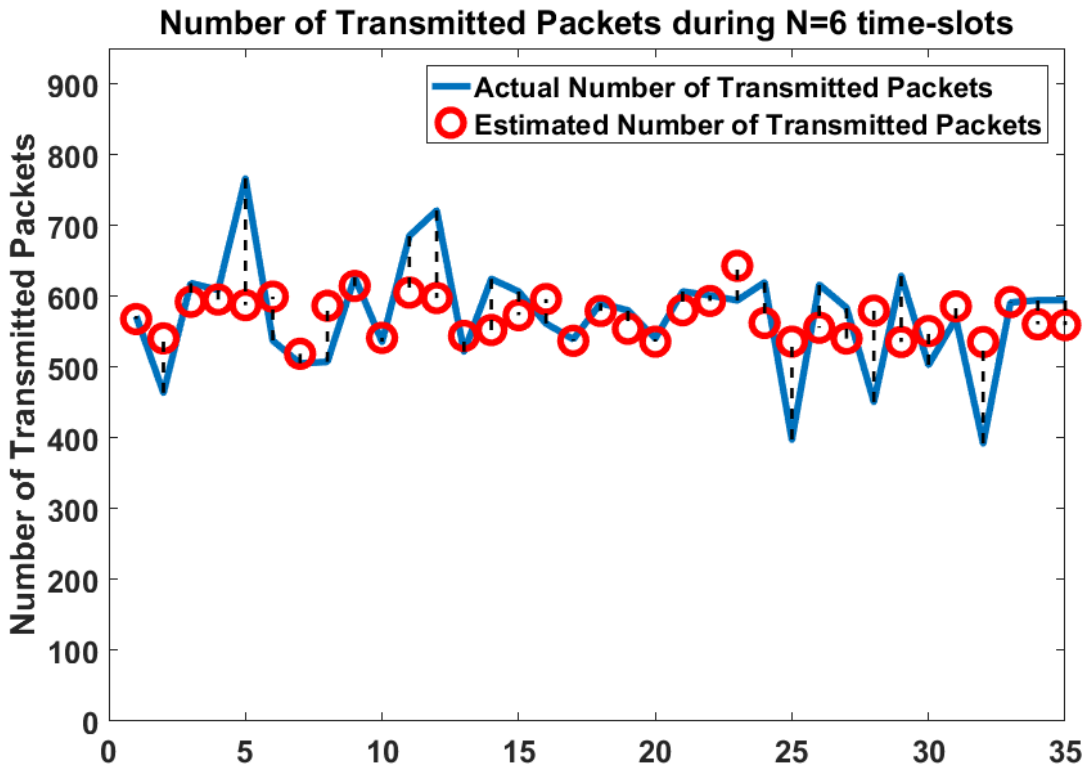

Figure 5.2: A simulation sample to illustrate the estimated number of packets to be transmitted during a scheduling period of $N = 6$ compared to the actual number of transmitted packets during a scheduling period of $N = 6$.

5.3. Performance Analysis and Discussion

In this section, the performance of the proposed opportunistic scheduling algorithm is evaluated. The performance evaluation results are found using Monte-Carlo simulations over the duration of 100,000 time-slots, and MATLAB is the program used to perform the simulations. Most of simulation parameters are in Table 5.1. The performance of the proposed opportunistic scheduling algorithm is compared to the performance of benchmark scheduling algorithm where $N = 1$. The performance metrics are the total number of transmitted packets every time-slot and the switching delay. Different traffic intensities for each SU can be assumed, but, for the sake of simplicity, the SUs activities are assumed to be equal and SU activities are set to $\pi_{active}^{SU} = 80\%$. Five PUs are licensed to five different channels. The PU activity of each channel is set to: 20%, 25%, 30%, 35%, and 40%, and five probability transition matrices of PU activities are found accordingly.

Table 5.1: Simulation parameters for the benchmark scheduling algorithm simulations.

Variable	Value
T	2 ms
B	5 bands
L	3 sub-channels per band
S	20 SUs
$\bar{\gamma}$	15 dB
m	1
PER_o	0.001
K	5 channel modes
f_d	50 Hz
W	6 MHz
t^{sen}	0.5 ms
t^c	0.5 ms
v^{sw}	0.1 ms/MHz
R_b	2 Mbps
L_p	1080 bits

First, the estimation process is investigated. The aim here is to study the accuracy of the estimation process. Figure 5.2 illustrates a sample of the simulation performed. Figure 5.2 shows the actual number of transmitted packets during the scheduling period, which is $N = 6$ is figure's case, compared to the estimated number of packets to be transmitted during scheduling period of $N = 6$. It can be seen that the estimation values are close to the actual number of transmitted packets. However, to fairly study the accuracy of the estimation process, the error between the estimated values and the actual results need to be investigated. The percentage error is found using the standard estimation error formula:

$$e_{est} = \left| \frac{\widetilde{R}_t - R_t}{R_t} \right| 100\%, \tag{5.15}$$

where $\widetilde{R}_t$ is the estimated number of transmitted packets during the whole scheduling period t and R_t is the actual number of transmitted packets during the whole scheduling period t. Figure 5.3 illustrates how scheduling periods effect estimation error under different Doppler frequencies. As shown Figure 5.3, in general, the estimation error decreases as scheduling periods increase. This happens due to the fact that as scheduling period increases, the actual number of transmitted packets during the scheduling period

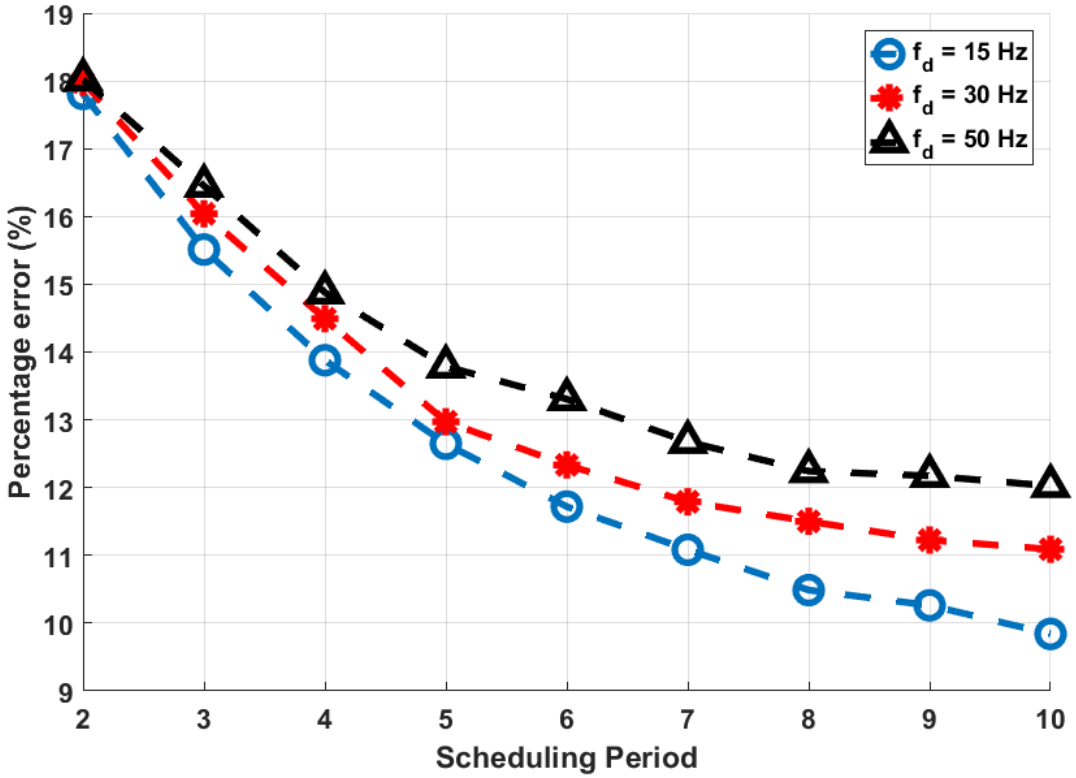

Figure 5.3: Estimation error percentage of the proposed opportunistic scheduling algorithm against scheduling period for different Doppler frequencies f_d.

tends to approach the expected value found by estimation algorithm. The error occurs because the dynamic behavior of the system affects the actual number of transmitted packets every time-slot. Recall that the number of transmitted packets depends on three main factors: channel occupancy, SU activity, and channel quality. Additionally, it is also assumed that when a SU is scheduled to a sub-channel, then the sub-channel will be assigned to that SU for the whole scheduling period N. Hence, if a major change occurred to system parameters, then the SU is forced to stick with its scheduled sub-channel. For example, if the PU turned from idle to active, then the SU cannot utilize the sub-channel and it also cannot change its assigned sub-channel. Additionally, if the SU becomes idle, then sub-channel will not be assigned to a different SU. Such random behavior impacts the estimation process, especially on the short run or short scheduling periods. However, the impact of random behavior decays as scheduling period increases. Hence, the behavior of estimation error decreases as scheduling periods increase.

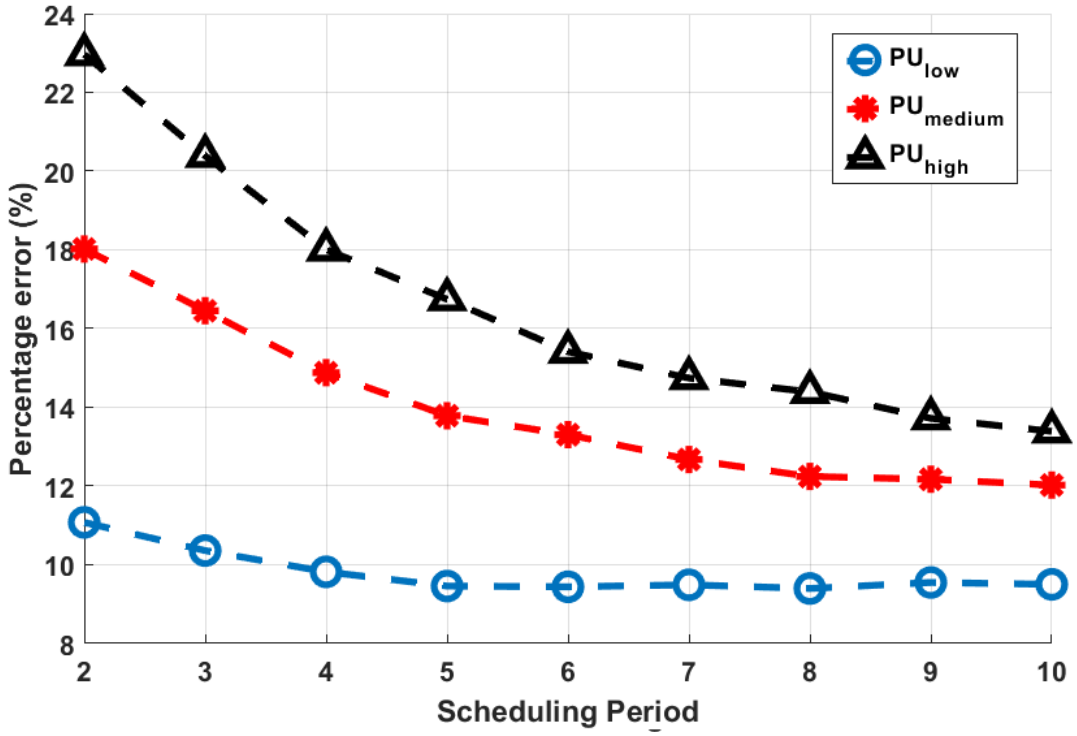

Figure 5.4: Estimation error percentage of the proposed opportunistic scheduling algorithm against the scheduling period for different PU activities.

The estimation error is investigated by varying the three mentioned factors: Doppler frequency, PU activity and SU activity. As mentioned earlier, Figure 5.3 shows how Doppler frequency or how the fading rates of the channel can affect the estimation error. As the Doppler frequency increases, the fading rates become higher and the channel becomes more dynamic. As a result, the channel will tend toward changing its current state instead of preserving it, thus heavily impacting the estimation accuracy and increasing the percentage error. On the other hand, if the channel is less dynamic, then it will tend toward preserving its current state rather than changing it. As a result, this will increase the accuracy of the estimation process, and it will reduce the percentage error. Figure 5.4, on the other hand, illustrates how the PU activity impacts the estimation process. PU activities used in the simulations are: $PU_{low}^{activity} = \{10\%, 10\%, 10\%, 10\%, 10\%\}$, $PU_{medium}^{activity} = \{20\%, 25\%, 30\%, 35\%, 40\%\}$, and $PU_{high}^{activity} = \{40\%, 40\%, 40\%, 40\%, 40\%\}$. From Figure 5.4, it can be shown that as the average PU activity of CRN increases, the percentage error increases. This happens because the increase in PU activity upsurges the unstability of the channel. Hence, resulting in more

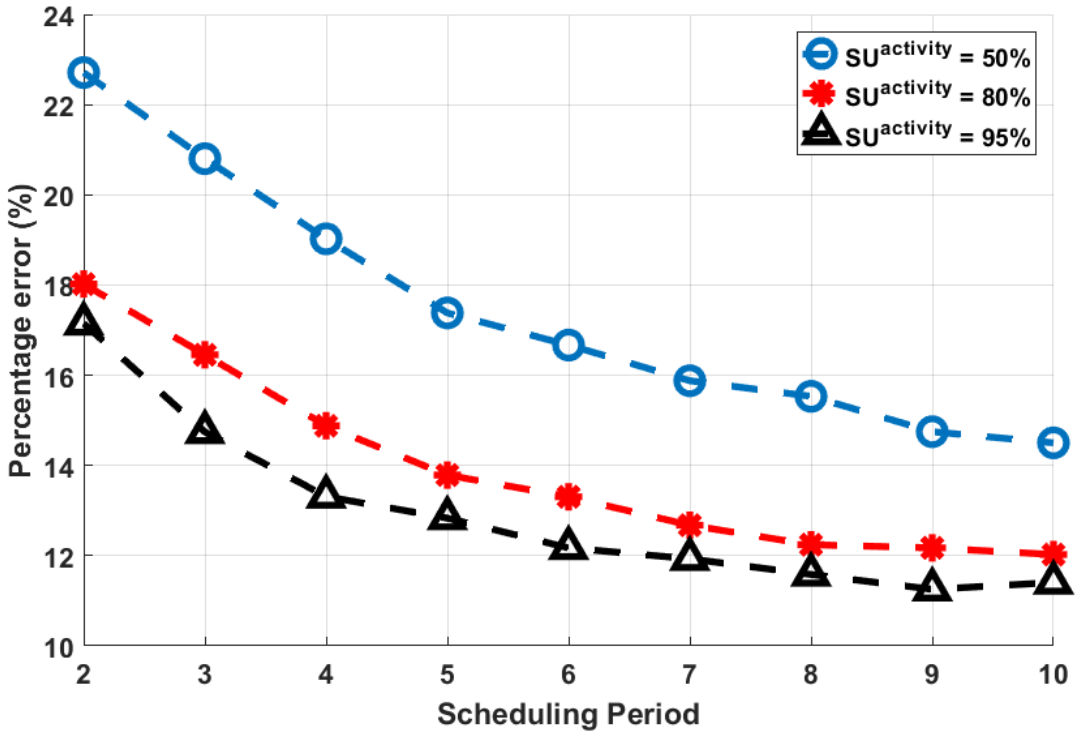

Figure 5.5: Estimation error percentage of the proposed opportunistic scheduling algorithm against the scheduling period for different SU activities.

changes in the spectrum occupancy and impacting the estimation accuracy. Additionally, if the PU activity decreases, then the changes in the spectrum decrease too, thus resulting in a more steady behavior and less error in the estimation process. Same argument applies to the relation between estimation error and the SU activity. Figure 5.5 demonstrates the relationship between the estimation accuracy and the SUs activities. As the SU activity gets higher, the SU tends to reserve its state toward being active, thus reducing the estimation error. However, when the SU activity is 50%, then the SU have 50-50% chance to either be active or idle, thus increasing the instability of the system. As a result, the error percentage will increase.

Moving forward, the performance of the proposed opportunistic scheduling algorithm is investigated. The performance measures are: the number of transmitted packets and switching delay. The number of transmitted packets in the CRN is calculated as:

$$\Upsilon_n = \sum_{j=1}^{BL} \sum_{s=1}^{S} X_n(j,s) R_n(j,s), \tag{5.16}$$

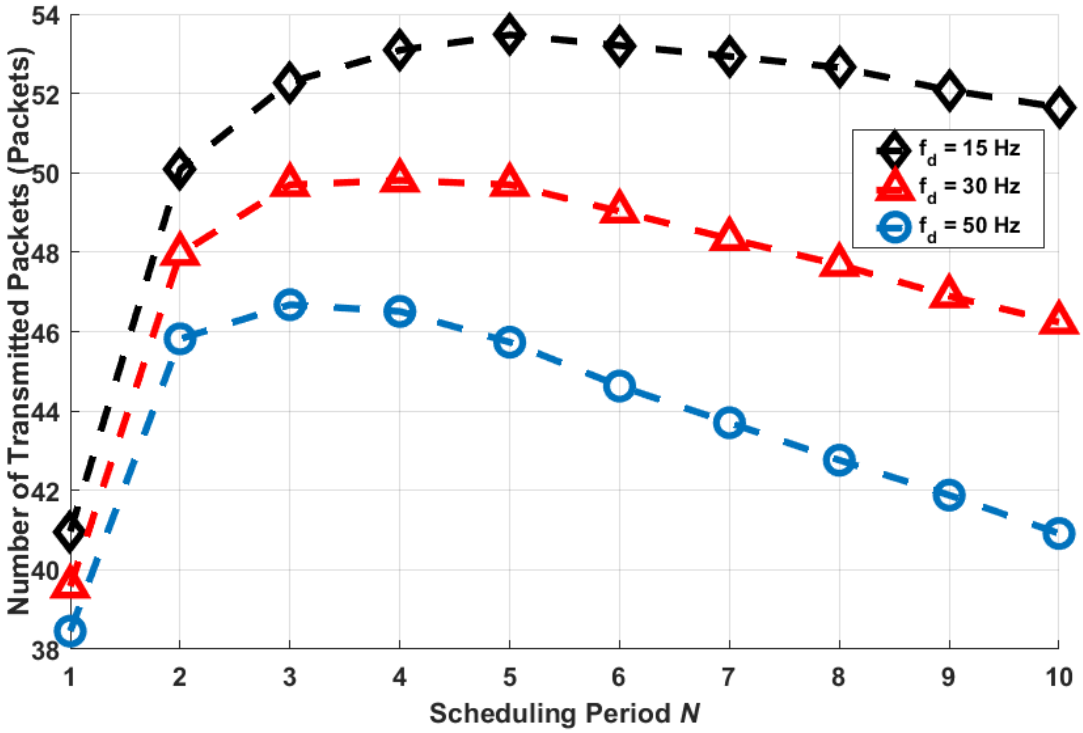

Figure 5.6: Average number of transmitted packets every time-slot in the CRN against the scheduling period for different Doppler frequencies f_d.

where $X_n(j,s) \in \{0,1\}$ is the decision variable of scheduling problem and $R_n(j,s)$ is the number of transmitted packets of SU s on sub-channel j at time-slot n and it is calculated:

$$R_n(j,s) = u_n(j)e_n(s)c_n(j,s)\left(\frac{R_b}{L_p}\right)t_n^{tr}. \tag{5.17}$$

The switching time per SU, on the other hand, is found as follow:

$$\tau_n = \frac{\sum_{s=1}^{S} X_n(s)t_n^{sw}(s)}{S}, \tag{5.18}$$

where $X_n(s) \in \{0,1\}$ is the decision variable of whether SU s is scheduled or not and $t_n^{sw}(s)$ is the switching time of SU s during time-slot n and it is found from:

$$t_n^{sw}(s) = v^{sw}\left|f_n^{new}(s) - f_n^{old}(s)\right|. \tag{5.19}$$

The effect of Doppler frequency on is investigated next. This will demonstrate how the performance of the scheduling algorithm varies with different fading rates. Recall

that the Doppler frequency indicates the fading rate of the channel, where high Doppler frequencies mean a dynamic channel and low Doppler frequencies represent less dynamic channels. As shown in Figure 5.6, the number of transmitted packets in the CRN does not reach its peak when the scheduling occurs every time-slot and the opportunistic scheduling algorithm does actually, in certain cases, increase the number of transmitted packets in theCRN. The benchmark scheduling algorithm does not achieve the maximum peak due to the bandwidth consuming effect of consecutive scheduling and switching that occur every time-slot. Moreover, the higher the fading rates, the more dynamic the system will become. As a result, the number of transmitted packets shows dependency on Doppler frequency where it is lower in high fading rate channels compared to low fading rate channels. This also explains the peak shift in the number of transmitted packets curves where the peak varies based on fading rates of the channel. The maximum number of transmitted packets when Doppler frequency is 50Hz is achieved when estimation is done over the span of $N = 3$ time-slots. As the Doppler frequency decreases and the channel becomes less dynamic, the maximum number of transmitted packets is achieved with higher scheduling periods. The maximum number of transmitted packets is achieved when $N = 4$ and $N = 5$ for Doppler frequencies 30Hz and 15Hz, respectively.

On the other hand, as shown in Figure 5.7, the switching delay increases as Doppler frequency increases. This happens because, in dynamic channels, the SU is expected to switch more frequently. Moreover, the switching delay has a decreasing behavior as N grows larger. This behavior is expected, since the main goal of this scheduler is to increase the bandwidth by reducing the effect of both switching and scheduling delays. Such behavior is dominant as scheduling periods get larger. On the other hand, scheduling every multiple time-slots can also cause an increase in switching delay. This occurs because increasing the scheduling period means that scheduling will only occur every N time-slots. Hence, the SU will not keep track of the changes occurring in the CRN, and during such time, the channel mode and system status can change drastically. Hence, in the next scheduling event, a lot of switching will take place in the CRN. The histogram in Figure 5.8 demonstrates such effect. As it can be seen, for $N = 1$ where scheduling occurs every time-slot, the switching delay of

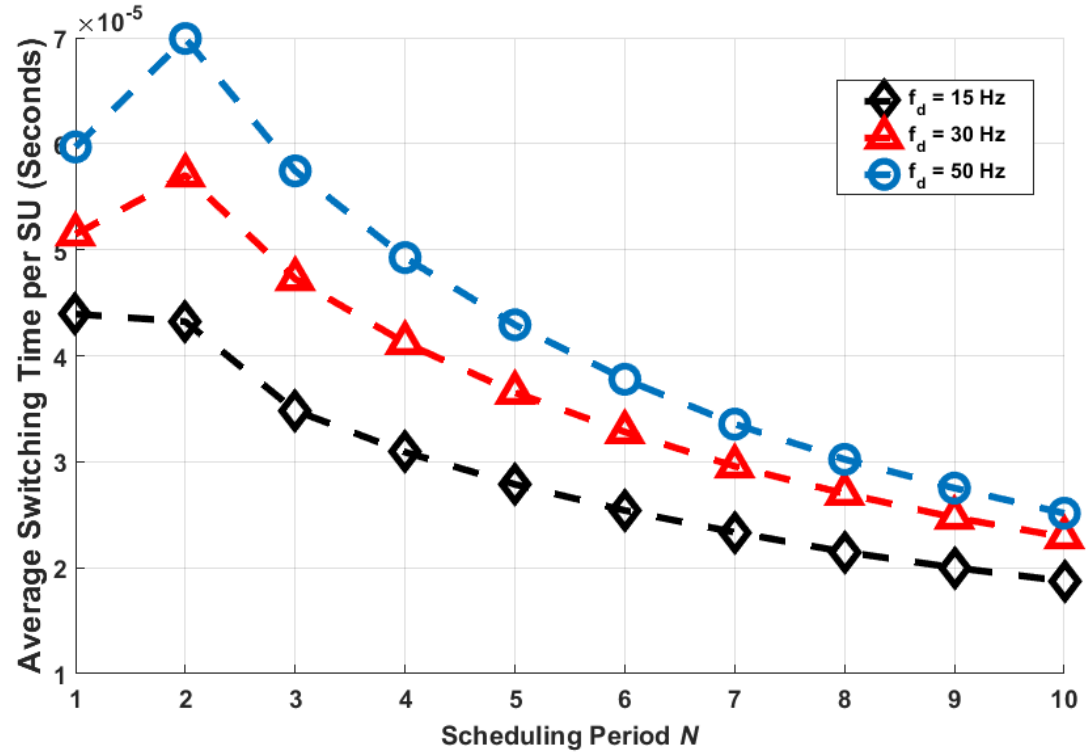

Figure 5.7: Average switching delay per SU every time-slot against the scheduling period for different Doppler frequencies f_d.

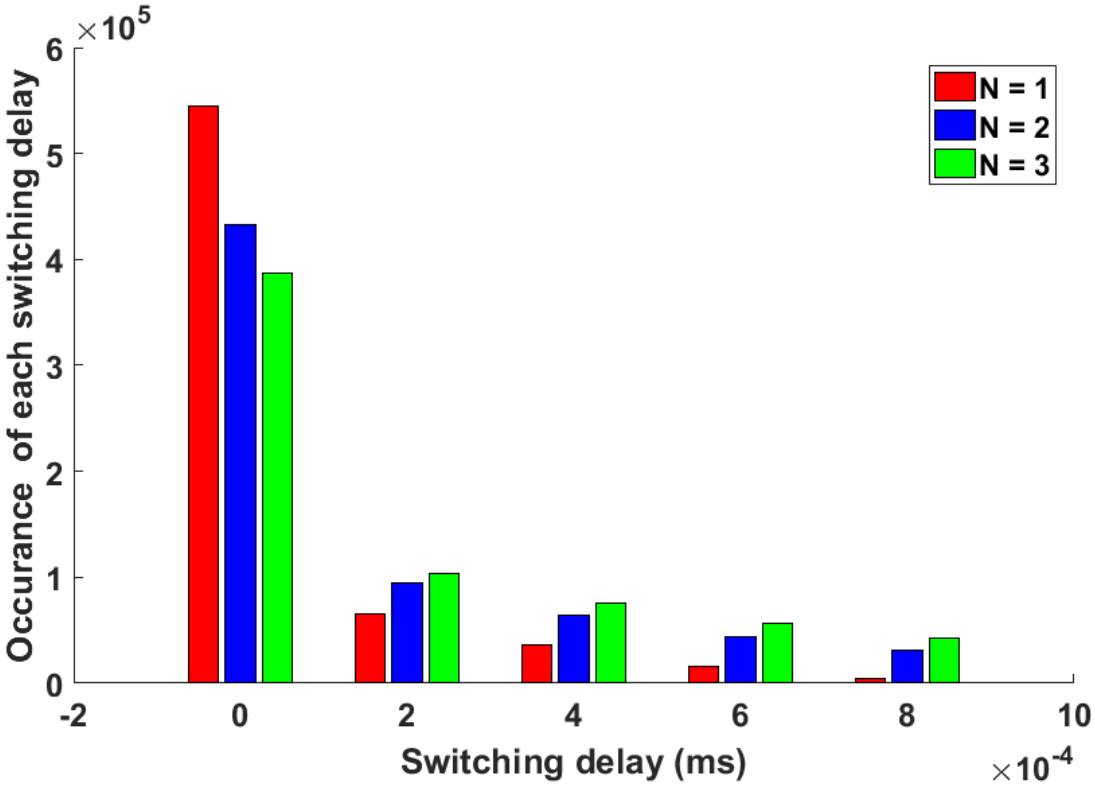

Figure 5.8: Histogram of occurrences of each switching delay for different scheduling periods N.

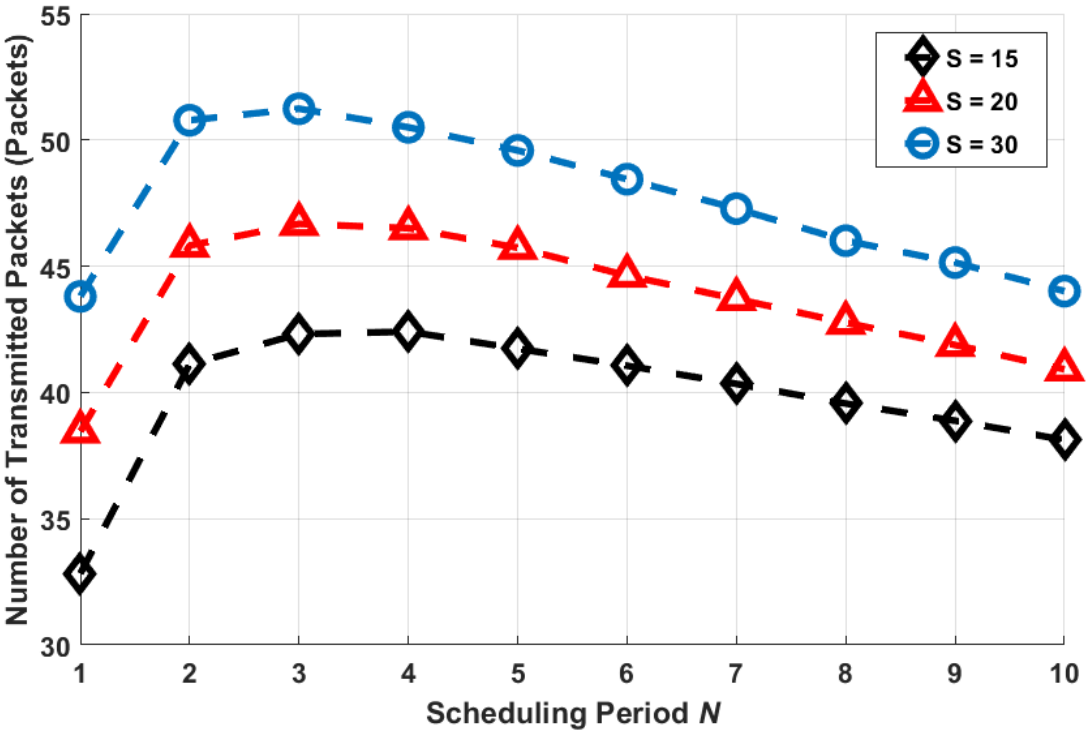

Figure 5.9: Average number of transmitted packets every time-slot in the CRN against the scheduling period for different numbers of SUs in the CRN.

SU tends to be zero and the mean of switching delay in the CRN is $6.1323 \times 10^{-2} ms$. Yet, when $N = 2$ or $N = 3$, the switching delays increase in the CRN where the mean of switching delays are $1.4451 \times 10^{-1} ms$ and $1.7876 \times 10^{-1} ms$ for $N = 2$ and $N = 3$, respectively. This behavior is dominant at small scheduling periods like $N = 2$ and $N = 3$. Yet, as N grows, this behavior gets dominated by reduced effect of scheduling and switching delays. Moreover, such behavior can be seen in a dynamic CRN because higher fading rates will result in an unstable system. From Figure 5.7, it can be seen that such behavior becomes stronger with high fading rates, as in $f_d = 50Hz$ curve, because the change in system parameter becomes more frequent, thus increasing the chances for SU switching in the CRN. Yet, when $f_d = 15Hz$ such behavior is not observable, due the less dynamic nature of the channel.

In the second set of simulations, the effect of SU's number on CRN performance is investigated. The Doppler frequency, in this simulation, is set to 50 Hz and the number of SUs in this simulation varies among $S \in \{15, 20, 30\}$. As illustrated in Figure 5.9, the number of transmitted packets in CRN increases as the number of SUs increases.

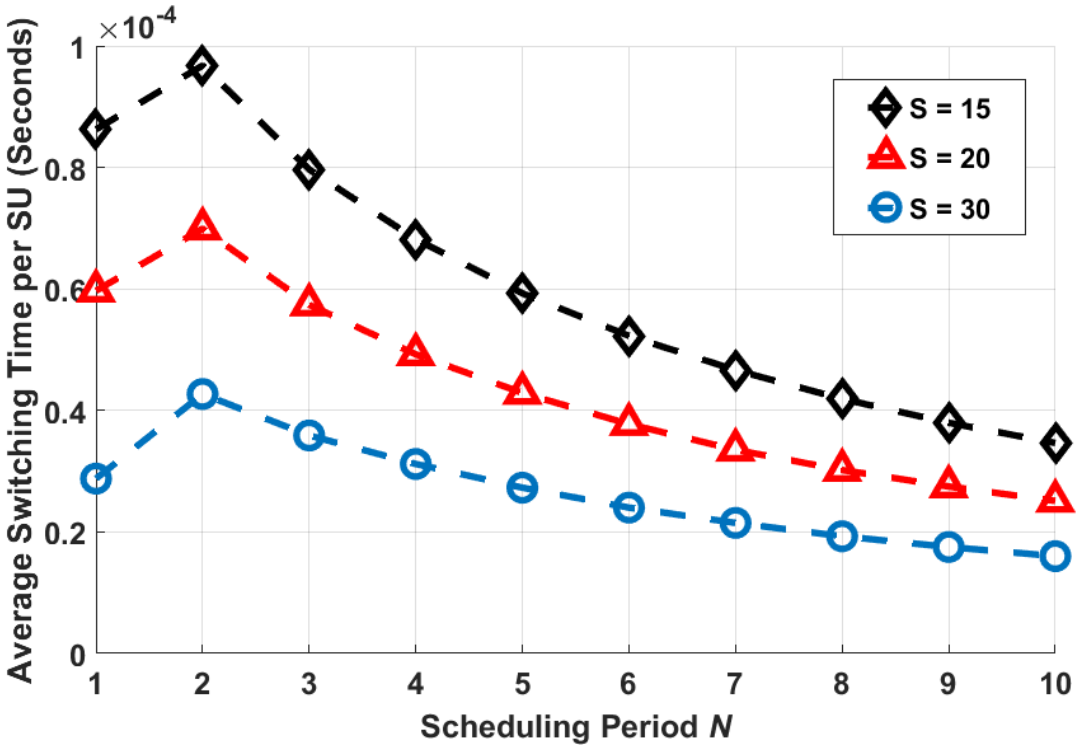

Figure 5.10: Average switching delay per SU every time-slot against the scheduling period for different numbers of SUs in the CRN.

Additionally, it can be noticed that this increase is a logarithmic increase since it slows when S becomes larger. This happens because the CRN resources are limited. Thus, as the number of SUs becomes larger, the spectrum cannot cope with the increasing demand of CRN and only a certain amount of SUs will be scheduled. From Figure 5.9, we can also notice that the maximum number of transmitted packets in the network occurs when the scheduling period is $N = 3$ and the peak does not depend on the number of SUs in the CRN. On the other hand, the switching time per SU, as shown in Figure 5.10, increases as the number of SUs in the CRN decreases. This happens because with more SUs, every SU will have less chances to transmit, hence causing less switching delay for each user.

In the last set of simulations, the effect of switching-delay latency factor, v^{sw}, on the number of transmitted packets in the CRN and switching delay per SU is studied. The Doppler frequency in this simulation is set to 50 Hz and the number of SUs is set to 20 users. As illustrated in Figure 5.11, the number of transmitted packets shows dependency on the latency factor. The number of transmitted packets increases as the

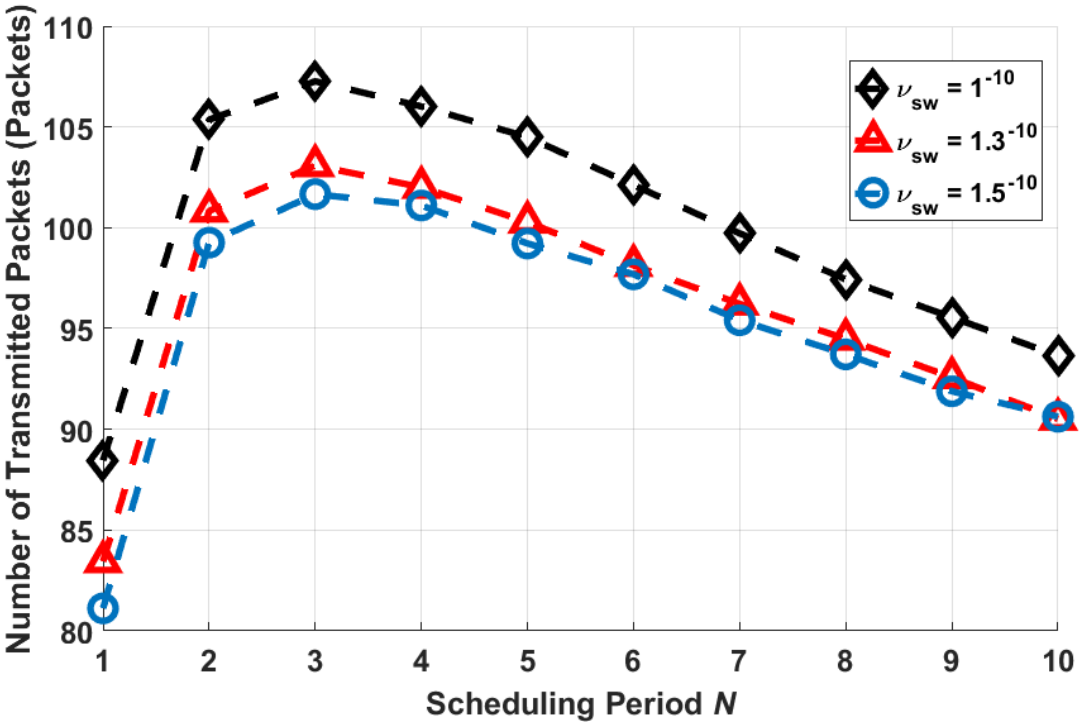

Figure 5.11: Average number of transmitted packets every time-slot in the CRN against the scheduling period for different latency factors v^{sw}.

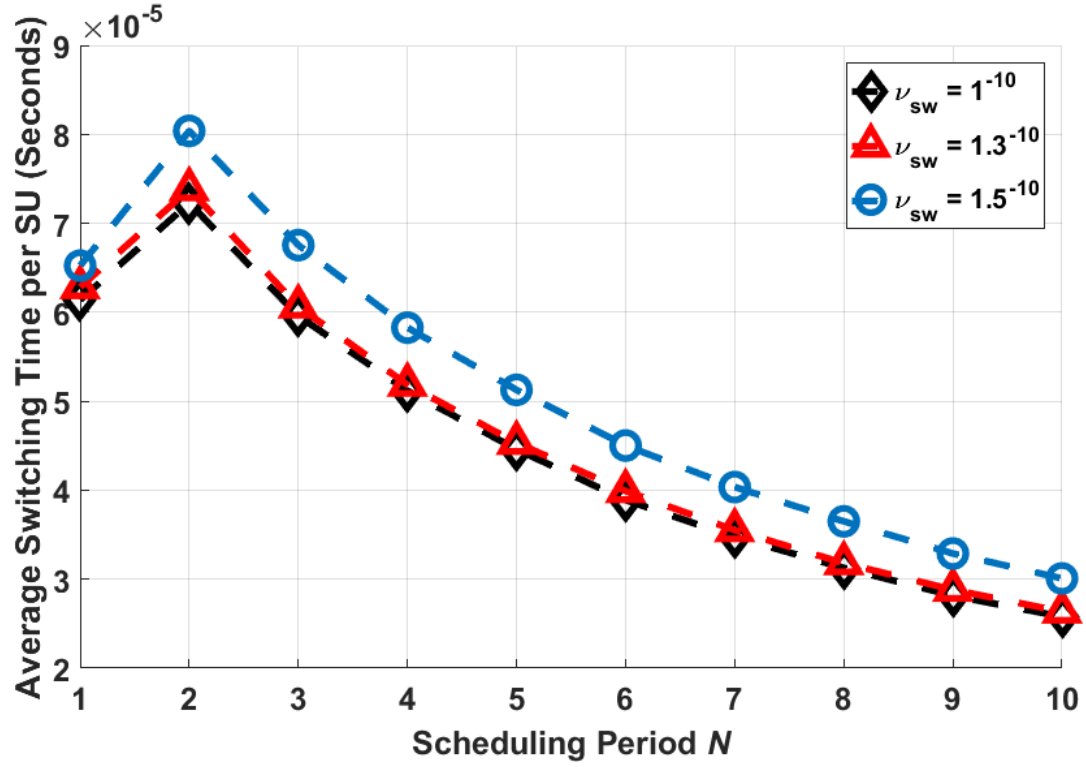

Figure 5.12: Average switching delay per SU every time-slot against the scheduling period for different latency factors v^{sw}.

latency factor decreases. That is due to the fact that, as the latency factor of switching-delay decreases, it allows the SUs to be scheduled into more sub-channels, because the smaller the latency factor, the less time it takes the SUs to switch sub-channels. Thus, increasing the range of sub-channels the SU can be scheduled to and reducing the switching-delay per channel. The maximum number of transmitted packets is achieved with $N = 3$, regardless of v^{sw}. Finally, Figure 5.12 shows that the switching delay is less with lower latency factors v^{sw} and that's because the lower the switching-delay factor, the less time it takes to switch among sub-channels.

Chapter 6: Interleave Scheduling Algorithm

As discussed in Chapter #4, SUs with small switching delay require large, heavy and costly equipments which is inefficient. Moreover, SUs with large switching delay will cause a degradation in the CRN performance since switching delay is a bandwidth consuming factor. Additionally, with the growth of CR concept in IoT and WSN, especially in commercial devices, SU electronics' cost became an important and decisive factor in designing SUs and CRNs. Moreover, new spectrum bands are being utilized, thus increasing the exploited spectrum range. As a result, switching delay is also a very crucial factor in the CRN. Recall, the switching time occurs because SUs are required to adjust their transceivers to operate on the new scheduled sub-channel or frequency [45]. As mentioned earlier in Subsection #4.1.3, the switching delay depends mainly on the current sub-channel and the new scheduled sub-channel. So, if the SU is scheduled to a new sub-channel, then it will need time to switch to new sub-channel. During this switching time, the new scheduled channel will be idle and underutilized. Therefore, the aim of the proposed scheduling algorithm in this chapter is to reduce the effect of the switching delay by utilizing it. The utilization is done by allowing other active and unscheduled SUs to transmit during the switching time of other scheduled SUs as shown in Figure 6.1. This interleaving process reduces the wasted bandwidth by allowing other SUs to exploit it. Henceforth, the proposed algorithm is referred to as interleave scheduling algorithm. Beside utilizing the wasted bandwidth, another advantage of the proposed scheduler is that it allows more SUs to transmit and exploit the spectrum. Unlike the benchmark scheduling algorithm, the maximum number of SUs that can exploit the system depends on the available resources or idle sub-channels. Hence, the maximum number of SUs to be scheduled is bounded by the number of available sub-channels $\left(S_n^{sch} \leq \chi_n \leq LB\right)$. Unlike the benchmark algorithm, in the interleave scheduling algorithm, the number of scheduled SUs is not bounded by the number of available sub-channels but by twice that number $\left(S_n^{sch} \leq 2\chi_n \leq 2LB\right)$. The extreme case occurs if all sub-channels are available and all SUs are scheduled to new sub-channels, then there will be another LB possible chances to transmit. It is worth mentioning that in this scheduling algorithm, the scheduling process is performed every time-slot. Therefore,

Figure 6.1: Illustration example of the interleave scheduling algorithm and how it utilizes the switching delays in CRN.

unlike the previous scheduler where the effect of both scheduling and switching delay reduced, the interleave scheduling algorithm only reduces the effect of switching delay.

6.1. Scheduling Algorithm

As mentioned before, the aim of the interleave scheduler is to utilize the switching delay by allowing other unscheduled SUs to transmit during it, which will reduce the effect of switching delay. Based on the histogram for $N = 1$ in Figure 5.8, the SUs tend to stay on their current channel for approximately 81% of the time, and switch-

ing occurs on approximately 19% of the time. Of course, such percentage depends on the system parameters: PU activity, SU status, and channel state. As shown in Figure 6.1, the interleave scheduler should seize the opportunity to allow other active SUs to transmit if possible. Note that Figure 6.1 is provided just for the sake of demonstrating and illustrating the idea behind the proposed scheduler. From Figure 6.1, we can see that both SU-3 and SU-5 are scheduled to stay in their channels. Thus, no switching delay will occur. On the other hand, SU-1, SU-2, and SU-7 are assigned to new channels. Hence, a switching delay will occur. Moreover, SU-4, SU-6, SU-8, and SU-9 are active and are not scheduled. Therefore, they can be scheduled to any possible opportunity for transmission and they are called candidate SUs, where Λ_n^{can} represents set of candidate SUs at time-slot n. The sub-channels assigned to SU-1, SU-2, and SU-7 are sub-channels 3, 6, and 9, respectively. These sub-channels are available to any SU in Λ_n^{can} to exploit, if possible. Such sub-channels are referred to as candidate sub-channels of second type. The set of candidate sub-channels of second type at time-slot n is denoted by Ω_n^{can}. As illustrated in Figure 6.1, SU-4, and SU-9 were able to exploit the available resources where it seems that the transceiver of SU-9 was already set on sub-channel 9. Hence, allowing SU-9 to utilize sub-channel 9 till SU-7 is able to use it. Simultaneously, it seems that the transceiver of SU-4 was adjusted to a frequency near available sub-channel 6, thus allowing it to exploit it. As it can be seen, the interleave scheduling algorithm is actually composed of two scheduling problems. The first scheduling problem is the benchmark scheduling problem discussed in Section #4.2. The second scheduling process is the interleave phase as illustrated in Figure 6.2. The second interleave phase is similar to benchmark scheduling process. However, it is done on the candidate SUs Λ_n^{can} and candidate sub-channels of second type Ω_n^{can}.

To perform the interleave scheduling algorithm, the first step is to perform the benchmark algorithm. Afterward, the goal is to find the set of candidate sub-channels of second type Ω_n^{can} and set of candidate active SUs Λ_n^{can}. Then, the number of transmitted packets of each candidate SU at each of the candidate sub-channel of second type is found as:

$$\check{R}_n(\omega,\lambda) = u_n(\omega)e_n(\lambda)Y_n(\omega,\lambda)\widetilde{t_n^{tr}}(\omega,\lambda), \tag{6.1}$$

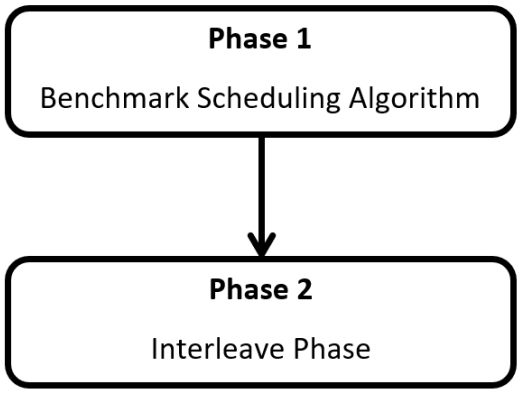

Figure 6.2: The two phases of the interleave scheduling algorithm.

where $\omega \in \Omega_n^{can}$, $\lambda \in \Lambda_n^{can}$, $\widetilde{t_n^{tr}}(\omega,\lambda)$ is the transmission time available for candidate user λ to transmit on sub-channel ω, $u_n(\omega)$ and $e_n(\lambda)$ are the PU activity and the SU status, respectively, and $Y_n(\omega,\lambda)$ represents the amount of packets that SU λ is transmitting on sub-channel ω at time-slot n, and can be found [41]:

$$Y_n(\omega,\lambda) = \left(\frac{R_b}{L_p}\right) c_n(\omega,\lambda). \tag{6.2}$$

As illustrated in Figure 6.3, the time to transmit $\widetilde{t_n^{tr}}$ is found by:

$$\widetilde{t_n^{tr}}(\omega,\lambda) = \max\left(0, T^{av}(\omega) - \widetilde{t_n^{sw}}(\omega,\lambda)\right), \tag{6.3}$$

where $\widetilde{t_n^{sw}}(\omega,\lambda)$ is the switching time of SU λ to sub-channel ω, and $T^{av}(\omega)$ is the available time for transmission on sub-channel ω which equals to $t_n^{sw}(\omega,s)$, switching delay of SU $s \in S_n^{sch}$ in sub-channel ω. It is possible for the switching delay to be more than the available time to transmit. This case happens if $T^{av}(\omega) < \widetilde{t_n^{sw}}(\omega,\lambda)$, and it will result in a negative transmission time $\widetilde{t_n^{tr}}(\omega,\lambda) < 0$. Therefore, the max(.) function is used to account for such cases. After finding $\check{R}_n(\omega,\lambda)$, the scheduling process is performed. Similar to the benchmark scheduling algorithm, the main objective of scheduling algorithm of second interleave phase is to maximize the total number of transmitted packets in the CRN. The optimization problem is formulated and it is a binary integer problem. The scheduling problem is performed every time-slot. From the definition, it can be seen that if the SU is not active or if the channel is occupied, then

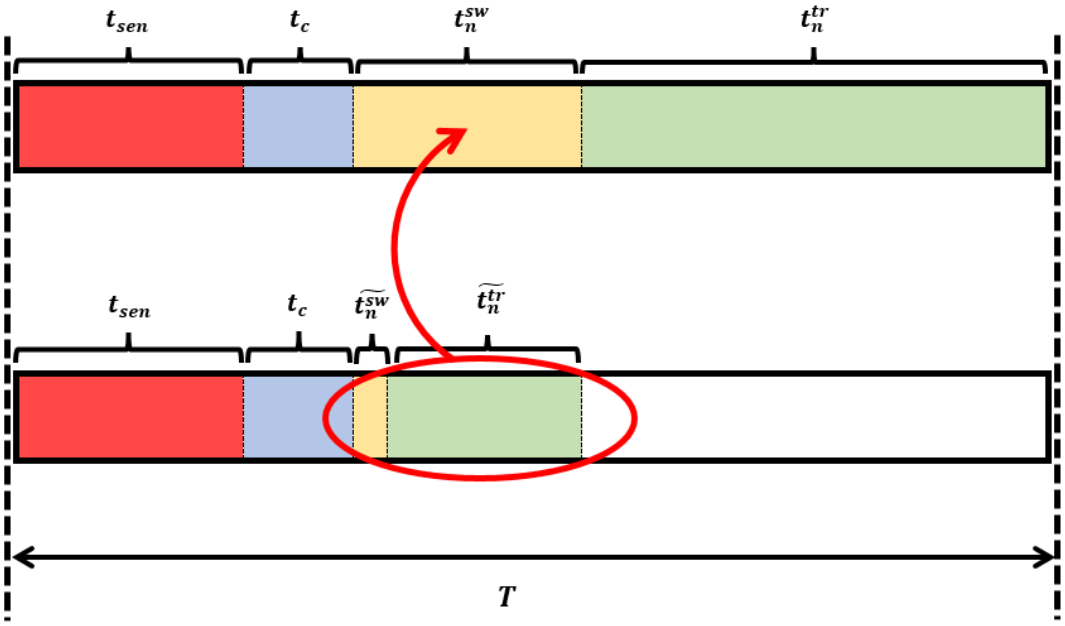

Figure 6.3: The MAC framework time notations during the interleave scheduling algorithms.

the number of transmitted packets will be zero. Additionally, if the transmission time is zero, then the amount of packets transmitted will also be zero. The CS needs to also take into consideration some predetermined constraints. The optimization problem is formulated as follow:

$$\max_{\vec{X}_{Int}} \quad \sum_{\omega=1}^{\Omega_n^{can}} \sum_{\lambda=1}^{\Lambda_n^{can}} X_{Int}(\omega,\lambda)\check{R}_n(\omega,\lambda), \tag{6.4}$$

$$\text{subject to} \quad X_{Int}(\omega,\lambda) \in \{0,1\}, \tag{6.5}$$

$$\sum_{\omega=1}^{\Omega_n^{can}} X_{Int}(\omega,\lambda) \leq 1, \quad \lambda \in \left\{1,\cdots,\Lambda_n^{can}\right\}, \tag{6.6}$$

$$\sum_{\lambda=1}^{\Lambda_n^{can}} X_{Int}(\omega,\lambda) \leq 1, \quad \omega \in \left\{1,\cdots,\Omega_n^{can}\right\}, \tag{6.7}$$

where $X_{Int}(\omega,\lambda)$ is the binary decision variable of second scheduling phase. Even though the scheduling problem for the second phase is similar to first phase. Yet, it is smaller in size, since the number of candidate SUs is less than or equal to active SUs $\left(\Lambda_n^{can} \leq S_{act}\right)$ and candidate sub-channels of second type are also less than or equal to

candidate sub-channels $\left(\Omega_n^{can} \leq \chi_n\right)$. In addition, the interleave scheduling algorithm has the same complexity $O\left(f(x)\right)$ as the benchmark scheduling algorithm. Since the scheduling phases in the interleave scheduling algorithm are consecutive and since they have the same complexity, then the scheduling algorithm complexity is $O\left(2f(x)\right) = O\left(f(x)\right)$. This is also another great advantage of the proposed algorithm in addition to the increase in the amount of transmitted information and the increase in the number of scheduled SU, which is that it has the same complexity as benchmark algorithm.

6.2. Comments on Optimization of the Proposed Scheduling Algorithm

The idea behind this chapter is to implement a scheduler that utilizes the switching delay by allowing active and unscheduled SUs to transmit during it. The scheduling problem aims to maximize the total number of transmitted packets in the CRN during a time-slot. Even though the proposed algorithm consists of two optimized scheduling algorithms. Yet, the proposed scheduler is a heuristic scheduling algorithm and it is not an optimized scheduling algorithm. Such optimization problem will be subjected to the following constraints. The first constraint is to permit only one active SU to transmit and use only one sub-channel at any point of time. Thus, more than one SU can utilize the sub-channel during any time-slot, but in a consecutive manner. In other words, more than one SU can utilize the channel, yet, they cannot do it simultaneously and they need to take turns utilizing it. The second constraint must be for any sub-channel to be granted to only a single SU at any point of time. In other words, the sub-channel can to be granted to more than one SU during time-slot, but in a consecutive manner. As a result, more than one decision variable need to be used. Such optimization problems are difficult to formulate. Therefore, the questions that should be asked before trying to bid on this approach are: Is it worth it? Will the CRN performance or amount of transmitted packets gain a huge boost? and are the benefits of such approach worth the costs? As discussed earlier, according to Figure 5.8, the scheduler tends to keep SUs in their assigned sub-channels for approximately 81% of the time. This is due to the fact that the cost required to switch sub-channels is bandwidth waste. Hence, SUs are mainly scheduled to new sub-channels whenever the channel that they are using becomes busy,

Table 6.1: Simulation parameters for the interleave scheduling algorithm simulations.

Variable	Value
T	3 ms
B	5 bands
L	3 sub-channels per band
S	20 SUs
$\bar{\gamma}$	15 dB
m	1
PER_o	0.0001
K	5 channel modes
f_d	50 Hz
W	6 MHz
t^{sen}	0.5 ms
t^c	0.5 ms
v^{sw}	0.1 ms/MHz
R_b	2 Mbps
L_p	1080 bits

SU becomes inactive, or when the channel mode gets low and other SUs have a better claim to the sub-channel. As a consequence, implementing such complicated optimized scheduling algorithm is inefficient. Moreover, the complexity of such problems is NP, if not NP-hard. Therefore, it is impractical and inefficient to solve such optimization problem in real-time. In such situations, greedy or heuristic algorithms, similar to the interleave algorithm discussed above, are used.

6.3. Performance Analysis and Discussion

In this section, the simulation results of the proposed interleave scheduling algorithm are demonstrated. Simulation parameters are illustrated in Table 6.1. Similar to previous simulations, the performance results are found using Monte-Carlo simulations over the duration of 100,000 time-slots, and MATLAB is the program used to perform the simulations. The performance of the interleave scheduling algorithm is compared to the performance of benchmark scheduling algorithm. The performance metrics are the total number of transmitted packets every time-slot and switching delay. Different traffic intensities for each SU can be assumed, but, for the sake of simplicity, the SUs activities are assumed to be equal and SU activities are set to $\pi_{active}^{SU} = 80\%$. Five

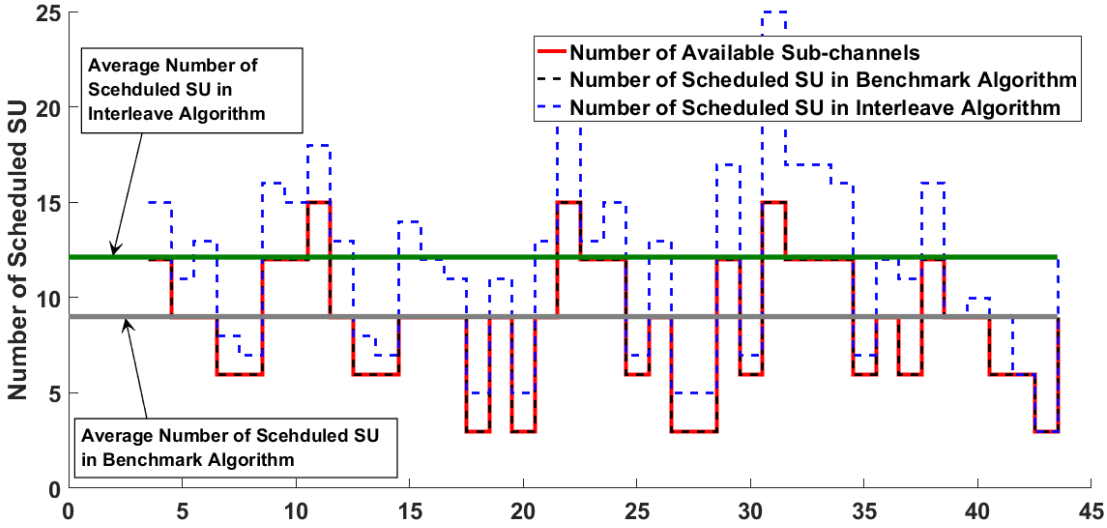

Figure 6.4: A simulation sample to illustrates the number of scheduled SUs in the CRN using the benchmark algorithm and the interleave algorithm over some time-slots.

PUs are licensed to five different channels. The PU activity of all channels are also set to be equal and they are set to high activity rate $\pi_{active}^{pu} = 40\%$ where PUs activities are: 40%, 40%, 40%, 40%, and 40%, and five probability transition matrices are found accordingly.

First, the number of scheduled SUs is investigated. Recall that one of the great advantages of this scheduling algorithm is that the number of scheduled SUs is not bounded by number of available sub-channels. Figure 6.4 illustrates a sample of the number of scheduled SUs over some time-slots. From Figure 6.4, it can be seen that the number of scheduled SUs in the benchmark algorithm is always bounded by number of available sub-channels. Since the available sub-channels depend on activities of PUs, then, as the PUs activity increases, the average number of available sub-channels decreases. The average number of scheduled SUs in the benchmark algorithm is approximately 8.9972 and it is indicated in Figure 6.4 by the gray line. Additionally, the maximum number of scheduled SUs is 15 SUs, where such cases occur if all sub-channels are available and more than or exactly 15 SUs are active. However, in the interleaves scheduling algorithm case, the number of scheduled SUs is not bounded by number of available sub-channels as shown in Figure 6.4. The maximum number of scheduled SUs can approach up to double the number of available channels. Thus,

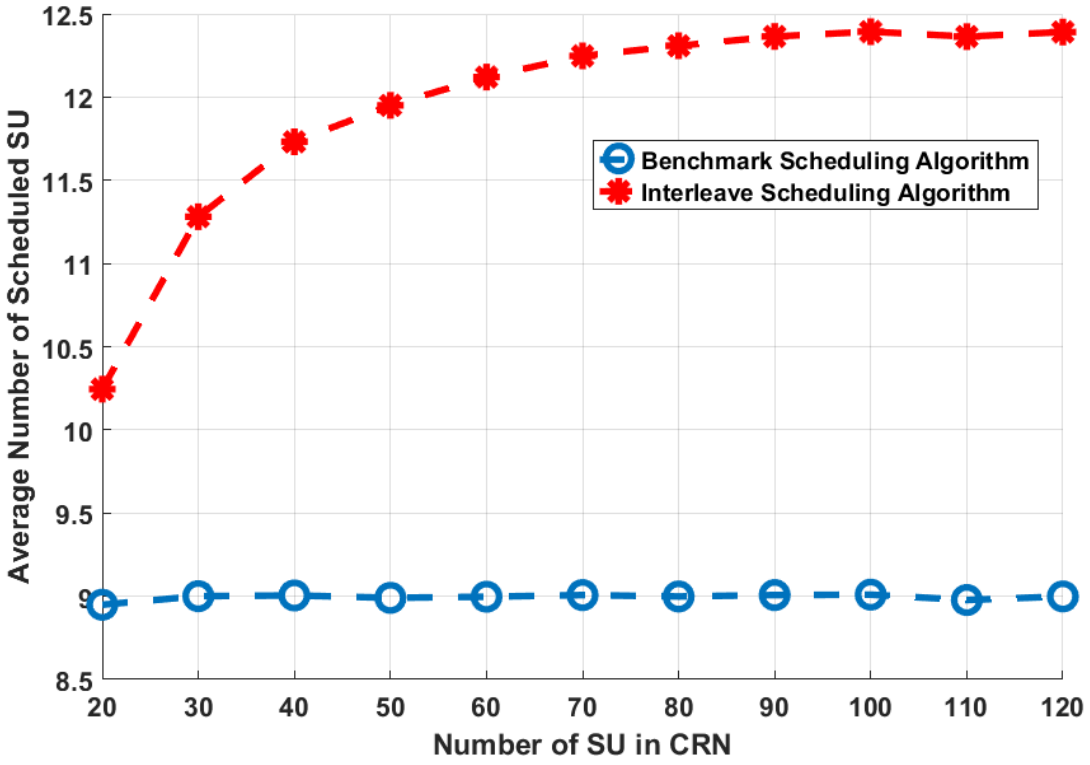

Figure 6.5: Average number of scheduled SUs in the CRN using the benchmark and interleave algorithms as functions of the number of SUs in CRN.

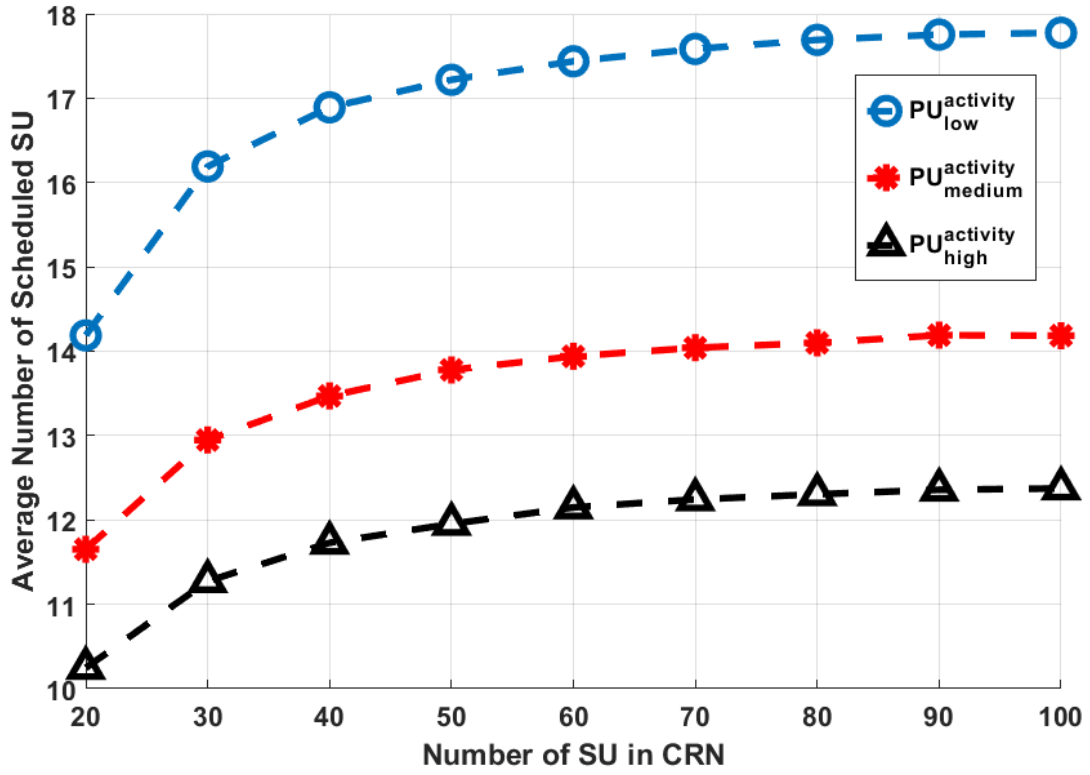

Figure 6.6: Average number of scheduled SUs in the CRN using the benchmark and interleave algorithms as functions of number of SUs in CRN for different PUs activities.

allowing more SUs to utilize the spectrum. The maximum number of scheduled SUs, in this simulation case, can reach up to 30 SUs. Additionally, the average number of scheduled SUs in the interleave scheduling algorithm is approximately 12.1206 which also depends on the availability of sub-channels or activity of PUs and it is indicated in Figure 6.4 by the green line. The number of scheduled SUs in the benchmark algorithm is calculated by:

$$S_n^{sch,Ben} = \sum_{s=1}^{S} X_n(s), \tag{6.8}$$

where $X_n(s)$ is the decision variable of whether SU s is scheduled or not. On the other hand, the number of scheduled SUs in the interleave scheduling algorithm is calculated by:

$$S_n^{sch,Int} = \sum_{s=1}^{S} X_n(s) + \sum_{s=1}^{S} X_n^{Int}(s), \tag{6.9}$$

where $X_n^{Int}(s)$ is the decision variable of the second interleave phase in the interleave scheduling algorithm. Figure 6.5 illustrates the number of scheduled SUs in both algorithms. As shown in Figure 6.5, the number of scheduled SUs in the benchmark scheduling algorithm is fixed and does not show any dependency on the number of SUs in the CRN. On the other hand, the number of scheduled SUs in the interleave scheduling algorithm increases as the number of SUs in CRN increases. This relation is explained by the fact that, as the number of SUs in the CRN increases, then the chances of SUs being candidates for the second interleave scheduling phase increases too. Henceforth, more SUs will be scheduled and have the chance to utilize the spectrum. Such growth is logarithmic in nature and such diminishing effect happens due to the limited spectrum and system resources. As a result, the average number of scheduled SUs will eventually reach a stationary value as the number of SUs grows in the CRN. Such stationary value depends mainly on the PU activity as illustrated in Figure 6.6. PU activities used in the simulations in Figure 6.6 are:$PU_{low}^{activity} = \{10\%, 10\%, 10\%, 10\%, 10\%\}$, $PU_{medium}^{activity} = \{20\%, 25\%, 30\%, 35\%, 40\%\}$, and $PU_{high}^{activity} = \{40\%, 40\%, 40\%, 40\%, 40\%\}$. Figure 6.6 shows that as the PU activity decreases, the stationary value of the number of scheduled SUs increases. This stationary value is bounded by $0 \leq S_n^{sch} \leq 2LB$ where $S_n^{sch} \to 0$ as $\pi_{active}^{PU} \to 100\%$ and $S_n^{sch} \to 2LB$ as $\pi_{active}^{PU} \to 0\%$. However, such cases are unrealistic because if $\pi_{active}^{PU} \to 100\%$, then there is no need to use CRN in the first

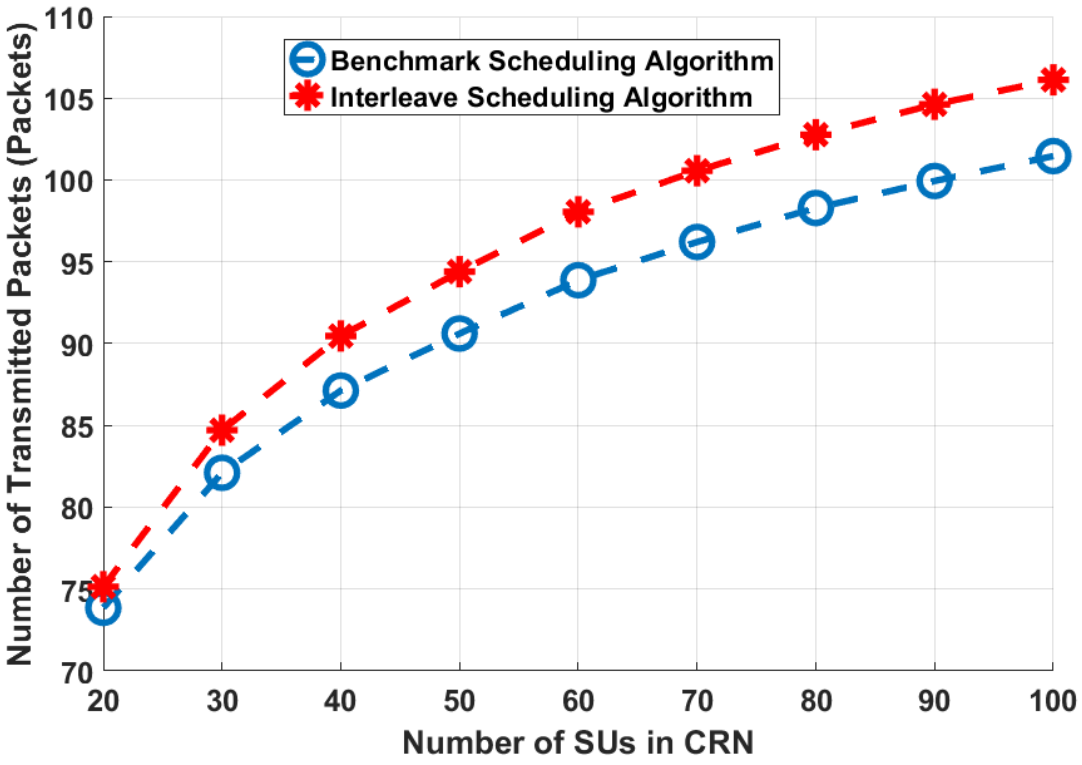

Figure 6.7: The number of transmitted packets every time-slot in the CRN using the benchmark and interleave algorithms as functions of the number of SUs in the CRN.

place, and if $\pi_{active}^{PU} \rightarrow 0\%$, then it might be better to use FSA to subscribers that can efficiently use the spectrum. The stationary value of the number of scheduled SUs does not depend on channel quality because the scheduling process mainly depends on the number of available sub-channels and the number of SUs in CRN, where the number of SUs in the CRN is correlated to the SU activity.

Moving forward, the amount of transmitted packets in the CRN is investigated. The number of transmitted packets in the CRN depends on a lot of factors and this value is calculated in the benchmark scheduling algorithm using Equations #5.16 and #5.17. Yet, in the interleave scheduling algorithm, it is found using:

$$\Upsilon_n = \sum_{j=1}^{BL} \sum_{s=1}^{S} X_n(j,s) R_n(j,s) + \sum_{j=1}^{BL} \sum_{s=1}^{S} X_n^{Int}(j,s) \check{R}_n(j,s), \tag{6.10}$$

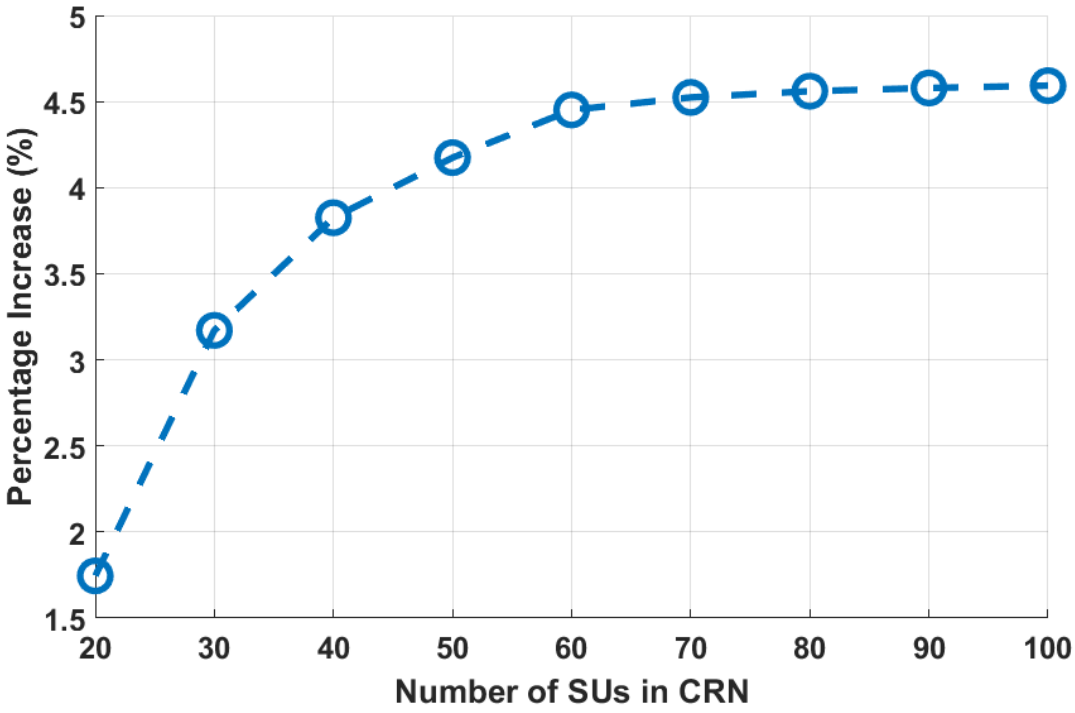

Figure 6.8: The increase percentage in the number of transmitted packets in the interleave scheduling algorithm compared to the benchmark scheduling algorithm as functions of the number of SUs in the CRN.

where $\check{R}_n(j,s)$ is the amount of transmitted packets by SU s on sub-channel j at time-slot n during the interleave phase and it is calculated:

$$\check{R}_n^{j,s} = u_n(j)e_n(s)c_n(j,s)\left(\frac{R_b}{L_p}\right)\widetilde{t_n^{tr}}(j,s). \tag{6.11}$$

Figure 6.7 illustrates the amount of transmitted packets in the CRN for both scheduling algorithms. The scheduling is done every time-slot. In general, the amount of transmitted packets increases, in both algorithms, as the number of SUs in the CRN increases. This is explained by the fact that, as the number of SUs increases, then more SUs will have the chance to transmit. However, such increase is logarithmic and that's due to the limited resources in the network. As shown Figure 6.7, the proposed interleave scheduling algorithm allows for more packets to be transmitted. This can be easily explained since the interleave scheduling algorithm consists of the benchmark scheduling algorithm and additional interleave phase to utilize the switching delay. Thus, the second phase is what made the difference, as it allowed for more active and unscheduled

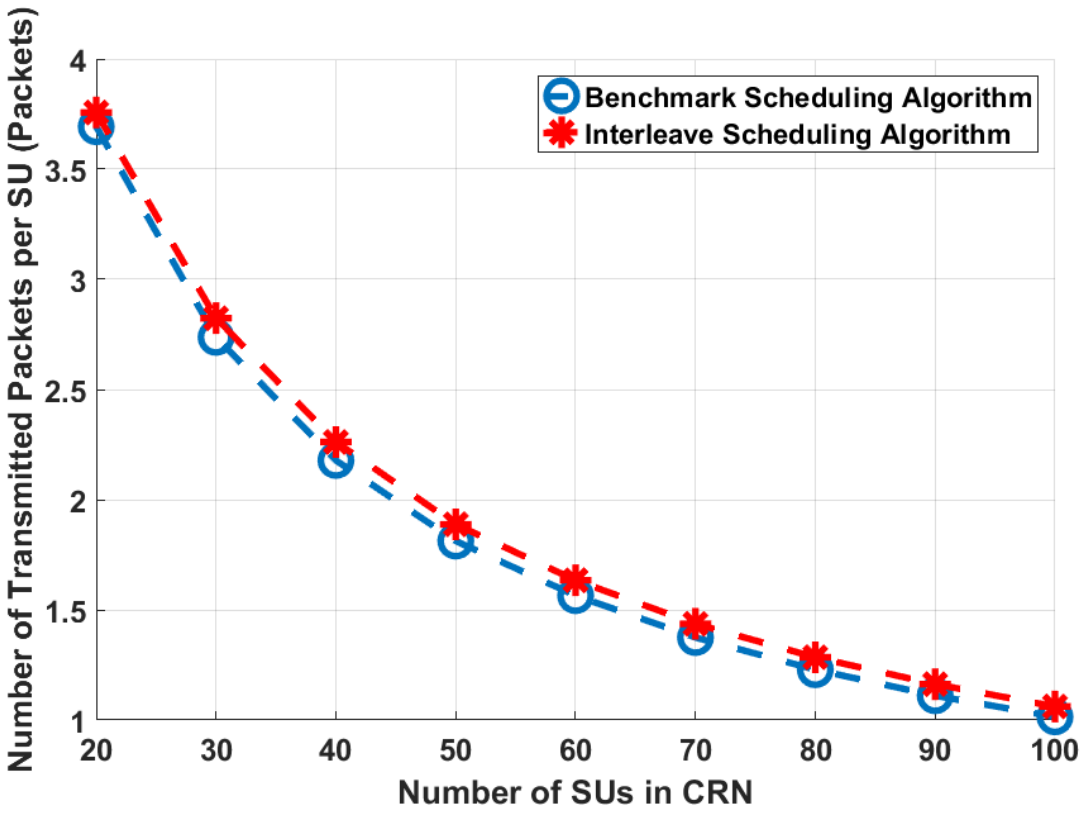

Figure 6.9: The number of transmitted packets per SU using the benchmark and interleave algorithms as functions of the number of SUs in the CRN.

SUs to transmit and utilize the spectrum. To study the increase in the amount of transmitted packets between the two algorithms, the increase percentage of the number of transmitted packets is:

$$\%increase = \frac{\left|\Upsilon_n^{Interleave} - \Upsilon_n^{Benchmark}\right|}{\Upsilon_n^{Benchmark}} \times 100\%. \tag{6.12}$$

Figure 6.8 illustrates the percentage increase in the number of transmitted packets and it shows that the interleave scheduling algorithm provides better performance compared to the benchmark algorithm. Such increase grows as number of the SUs increases and it is logarithmic in nature. The maximum increase percentage is approximately 4.5% and such value also depends on other factors such as: Doppler frequency and PU activity. The amount of transmitted packets per SU is also investigated in Figure 6.9. The

number of transmitted packets from each SU in the CRN is calculated using:

$$\rho_n^{Benchamrk} = \sum_{j=1}^{BL} X_n(j,s)u_n(j)e_n(s)c_n(j,s)\left(\frac{R_b}{L_p}\right)t_n^{tr}(j,s), \quad s \in S, \tag{6.13}$$

for the benchmark scheduling algorithm, and:

$$\begin{aligned}\rho_n^{Interleave} = \quad & \sum_{j=1}^{BL} X_n(j,s)u_n(j)e_n(s)c_n(j,s)\left(\frac{R_b}{L_p}\right)t_n^{tr} \\ & + \sum_{j=1}^{BL} X_n^{Int}(j,s)u_n(j)e_n(s)c_n(j,s)\left(\frac{R_b}{L_p}\right)\widetilde{t_n^{tr}}(j,s), \\ & s \in S,\end{aligned} \tag{6.14}$$

for the interleave scheduling algorithm. The average amount of transmitted packets of each SU is found by taking the mean of both $\rho_n^{Benchamrk}$ and $\rho_n^{Interleave}$ in respect to all SUs. As illustrated in Figure 6.9, the amount of transmitted packets per SU decreases as the number of SUs in the CRN increases. This can be explained by the fact that, in limited resources network, each SU will have fewer resources as the number of SUs in the CRN increase. Additionally, it can also be seen that the amount of transmitted packets of each SU in the interleave scheduling algorithm is greater compared to the benchmark scheduling algorithm. In other words, by using the interleave scheduling algorithm, the amount of transmitted packets of each SU will not be compromised when the number of SUs increases in the CRN.

Moving on, the switching time occurring in the CRN is found as follow:

$$\tau_n^{Ben} = \sum_{s=1}^{S} X_n(s)t_n^{sw}(s), \tag{6.15}$$

for the benchmark scheduling algorithm, and:

$$\tau_n^{Int} = \sum_{s=1}^{S} X_n(s)t_n^{sw}(s) + \sum_{s=1}^{S} X_n^{Int}(s)\widetilde{t_n^{sw}}(s), \tag{6.16}$$

for the interleave scheduling algorithm. Since more SUs are allowed to transmit during switching delay of first phase, there will be a slight chance that a SU switches its chan-

nel to seize such opportunities, thus causing more switching delay to occur. Therefore, the switching delay of the SUs in the CRN does not fairly represent how the interleave scheduling algorithm minimizes the effect of switching delay. As a result, a new performance measure is introduced. This new performance metric is called the effective switching time. Such metric represents the time that is actually wasted and not utilized during the switching phase and it is found using:

$$\widetilde{\tau}_n^{Eff} = \left(\sum_{s=1}^{S} X_n(s) t_n^{sw}(s) + \sum_{s=1}^{S} X_n^{Int}(s) \widetilde{t_n^{sw}}(s) \right) - \sum_{s=1}^{S} X_n^{Int}(s) \widetilde{t_n^{tr}}(s). \tag{6.17}$$

The above equation simply states that the underutilized switching delay is the transmission time of the second interleave phase subtracted from the switching delay of the first phase. In other words, the time that is being utilized during the second phase subtracted from the underutilized time of the switching delay. By doing so, we can capture the actual wasted switching delay. Figure 6.10 illustrates all the above switching delays in the CRN when both the benchmark and interleave algorithms are used. As illustrated, in general, the switching delay in the CRN decreases as the number of SUs in the CRN increases. This occurs because more SUs means that not all SUs will have the chance to transmit. This is due to the limited resources of the CRN. In addition, it can also be seen that the total switching delay occurring in the CRN, when the proposed interleave algorithm is used, is greater than the switching delay when the benchmark scheduling algorithm is employed. However, as mentioned earlier, to be able to utilize the switching delay of the first phase in the interleave scheduling algorithm, the SUs need to sometimes reallocate and switch their sub-channels to capture such transmission opportunities, hence resulting in a more switching delay. Thus, the switching delay is not sufficient to fairy show how the interleave algorithm reduces the switching delay effect. As a result, effective switching delay is used. As mentioned above, the effective switching delay captures the wasted time during switching delay of the first stage in the interleave algorithm. As demonstrated in Figure 6.10, the actual underutilized and wasted switching time is represented with effective switching delay blue curve. This shows that the interleave scheduling algorithm did actually reduce the effect of switching delay which allowed for less wasted bandwidth.

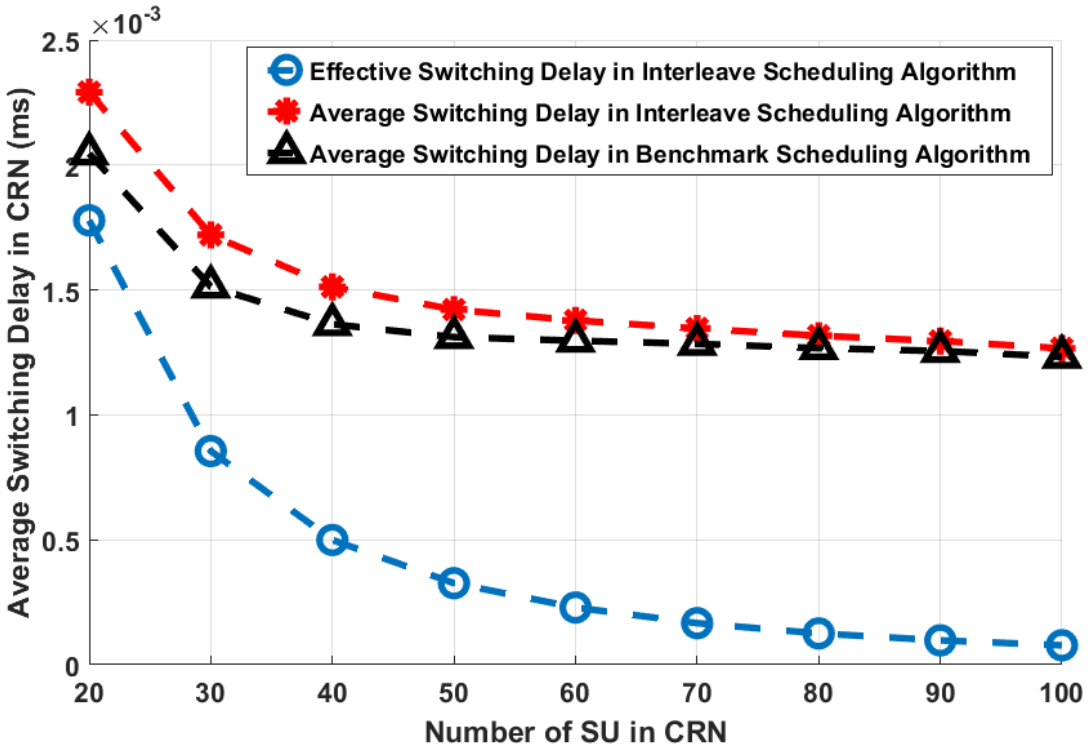

Figure 6.10: Average switching delays in the CRN using the benchmark and interleave algorithms as functions of the number of SUs in the CRN.

Chapter 7: Conclusion and Future Work

In this thesis, two dynamic spectrum scheduling and management techniques were proposed. The aim of these scheduling techniques is to maximize the total amount of transmitted information in the CRN while reducing the effect of switching delay. After modeling the system and the CRN, both scheduling algorithms are modeled and formulated. Monte-Carlo simulations were carried to study the behavior of the designed schedulers based on varying network's parameters. Afterward, a comparison between these scheduling algorithms and a benchmark scheduling algorithm was carried out based on the total amount of transmitted packets in the CRN and switching delay in the CRN. In addition, different performance metrics are also used to demonstrates the advantages on each scheduling technique. Moreover, the behavior of the designed schedulers under different scenarios and traffic loads are also investigated. From the simulation results, both of the implemented schedulers delivered a higher amount of transmitted packets compared to the benchmark scheduling algorithms and both schedulers were able to reduce the effect of switching delay.

The first algorithm is an opportunistic scheduling algorithm where scheduling is done every multiple time-slots. The scheduler, which was first proposed to reduce scheduling delay effect with a heuristic algorithm, was improve and modeled to reduce the effect both the scheduling and switching delays. Moreover, the scheduling process was done using an optimization algorithm and not a greedy algorithm as in previous work. The opportunistic scheduler showed better performance compared to the benchmark scheduling algorithm where the scheduling problem is done every time-slot. Additionally, the scheduler was able to deliver a higher amount of transmitted packets. Moreover, the scheduler was able to reduce the effect of both switching and scheduling delays.

On the other hand, the second scheduler is the interleave scheduling algorithm. The interleave scheduling algorithm was proposed in this thesis to minimize the switching delay by allowing other SUs to utilize it. The proposed algorithm allowed for more packets to be transmitted, reduced effect of switching delay, and allowed more SUs to utilize the spectrum. Moreover, the proposed scheduler has the same complexity as the

benchmark scheduling algorithm and scheduling is done every time-slot. As expected, it was observed that the interleave scheduler delivered a higher amount of packets by reducing the wasted bandwidth caused by switching delay, and allowed for more SUs to be scheduled.

Future work will include:

1. Developing a scheduler that takes into account other objective functions during the scheduling process such as: reducing the interference to other PUs and other SUs, ensuring fairness among CRN nodes, maintaining QoS requirement of different SUs traffic types, reducing end-to-end delay, and minimizing the SUs energy consumption.

2. Developing a more realistic model of SUs by including buffers for each SU and study the loss of each SU in terms of dropping probability and blocking probability.

3. Adding a more application specific SUs such as: VoIP or video streaming SUs, to the model.

4. Including the effect of imperfect sensing and study the effect of misdetection and false alarm probabilities on scheduler and CRN performance metrics.

5. Modifying the scheduling algorithms in this thesis to a distributed Ad-hoc CRN, and adding routing delay to switching delay effect.

References

[1] GSMA, "The mobile economy 2016," GSM Association, London, UK, Rep., 2016.

[2] R. van der Meulen. (2015, Nov.) Gartner says 6.4 billion connected things will be in use in 2016, up 30 percent from 2015. Internet. [Online]. Available: http://www.gartner.com/newsroom/id/3165317

[3] P. Rawat, K. D. Singh, and J. M. Bonnin, "Cognitive radio for M2M and Internet of Things: A survey," *Computer Communications*, vol. 94, pp. 1–29, Nov. 2016.

[4] J. Mitola and G. Q. Maguire, "Cognitive radio: Making software radios more personal," *IEEE Pers. Commun.*, vol. 66, no. 04, pp. 13–18, 1999.

[5] A. Agarwal, A. S. Sengar, R. Gangopadhyay, and S. Debnath, "A real time measurement based spectrum occupancy investigation in north-western india for cognitive radio applications," in *Proc. IEEE WiSPNET*, 2016, pp. 2035–2039.

[6] O. D. Babalola, E. Garba, I. T. Oladimeji, A. S. Bamiduro, N. Faruk, A. A. A. O. A. Sowande, O. W. Bello, and M. Y. Muhammad, "Spectrum occupancy measurements in the TV and CDMA bands," in *Proc. CYBER-ABUJA*, 2015, pp. 192–196.

[7] M. R. Dzulkifli, M. R. Kamarudin, and T. A. Rahman, "Spectrum occupancy at UHF TV band for cognitive radio applications," in *Proc. IEEE International RF and Microwave Conference*, 2011, pp. 111–114.

[8] "Federal Communications Commission, notice of proposal rulemaking and order," Federal Communications Commission, Washington, D.C., Rep. ET Docket No. 03-322, 2003.

[9] Y.-C. Liang, K.-C. Chen, G. Y. Li, and P. Mhnen, "Cognitive radio networking and communications: An overview," *IEEE Trans. Veh. Technol.*, vol. 60, no. 07, pp. 3386–3407, Sept. 2011.

[10] D. Gözüpek, S. Buhari, and F. Alagöz, "A spectrum switching delay-aware scheduling algorithm for centralized cognitive radio networks," *IEEE Trans. Mobile Comput.*, vol. 12, no. 07, pp. 1270–1280, July 2013.

[11] E. Ahmed, A. Gani, S. Abolfazli, L. J. Yao, and S. U. Khan, "Channel assignment algorithms in cognitive radio networks: Taxonomy, open issues, and challenges," *IEEE Commun. Surveys Tuts.*, vol. 18, no. 01, pp. 795–823, 2016.

[12] Y. Zhang, H. Lu, H. Wang, and X. Hong, "Cognitive cellular content delivery networks: Cross-layer design and analysis," in *Proc. Veh. Tech. Conf.*, 2016, pp. 1–6.

[13] J.-C. Liang and J.-C. Chen, "Resource allocation in cognitive radio relay networks," *IEEE J. Sel. Areas Commun.*, vol. 31, no. 03, pp. 476–488, Mar. 2013.

[14] V. K. Tumuluru, P. Wang, D. Niyato, and W. Song, "Performance analysis of cognitive radio spectrum access with prioritized traffic," *IEEE J. Sel. Areas Commun.*, vol. 61, no. 04, pp. 1895–1906, May 2012.

[15] S. Bayhan, S. Eryigit, F. Alagöz, and T. Tugcu, "Low complexity uplink schedulers for energy-efficient cognitive radio networks," *IEEE Wireless Commun. Lett.*, vol. 02, no. 03, pp. 363–366, June 2013.

[16] N. Shami and M. Rasti, "An energy efficiency scheduling scheme for cognitive radio networks," in *Proc. ICEE*, 2015, pp. 648–653.

[17] A. Homayounzadeh and M. Mahdavi, "Quality of service provisioning for real-time traffic in cognitive radio networks," *IEEE Commun. Lett.*, vol. 19, no. 03, pp. 467–470, Mar. 2015.

[18] Y. H. Chye, E. Dutkiewiczy, R. Vesilo, and R. P. Liu, "QoS-aware cross-layer scheduling for cognitive radio networks with heterogeneous data traffic," in *Proc. ATNAC*, 2013, pp. 213–218.

[19] M. A. Safwat, "Dynamic spectrum access with traffic prioritization in cognitive radio networks," in *Proc. ISNCC*, 2015, pp. 1–6.

[20] R. Doost-Mohammady, M. Y. Naderi, , and K. R. Chowdhury, "Spectrum allocation and QoS provisioning framework for cognitive radio with heterogeneous service classes," *IEEE Trans. Wireless Commun.*, vol. 13, no. 7, pp. 3938–3950, July 2014.

[21] S. Wang, Y. Wang, J. P. Coon, and A. Doufexi, "Energy-efficient spectrum sensing and access for cognitive radio networks," *IEEE Trans. Veh. Technol.*, vol. 61, no. 02, pp. 906–912, Feb. 2012.

[22] S. M. Kannappa, T. Ali, and M. Saquib, "Analysis of a buffered cognitive wireless network with dynamic spectrum assignment," in *Proc. IEEE ICC, Cognitive Radio and Networks Symposium*, 2014, pp. 1434–1440.

[23] M. Abdelraheem, M. J. Abdel-Rahman, M. El-Nainay, and S. F. Midkiff, "Spectrum-efficient resource allocation framework for cooperative opportunistic wireless networks," *'IEEE Trans. Cogn. Commun. Netw*, vol. 02, no. 03, pp. 249–261, Sept. 2016.

[24] Q. Jiang, V. C. M. Leung, M. T. Pourazad, H. Tang, and H.-S. Xi, "Energy-efficient adaptive transmission of scalable video streaming in cognitive radio communications," *IEEE Syst. J.*, vol. 10, no. 02, pp. 761–772, June 2016.

[25] N. Janatian, S. Sun, and M. Modarres-Hashemi, "Joint optimal spectrum sensing and power allocation in CDMA-based cognitive radio networks," *IEEE Trans. Veh. Technol.*, vol. 64, no. 09, pp. 3990–3999, Sept. 2015.

[26] Y. Wu, F. Hu, Y. Zhu, and S. Kumar, "Optimal spectrum handoff control for crn based on hybrid priority queueing and multi-teacher apprentice learning," *IEEE Trans. Veh. Technol.*, vol. PP, pp. 1–6, 2016.

[27] M. J. N. Oliaee, B. Hamdaoui, X. Cheng, T. Znati, and M. Guizani, "Analyzing cognitive network access efficiency under limited spectrum handoff agility," *IEEE Trans. Veh. Technol.*, vol. 63, no. 03, pp. 1402–1407, Mar. 2014.

[28] T. M. C. Chu, H. Phan, , and H.-J. Zepernick, "Dynamic spectrum access for cognitive radio networks with prioritized traffics," *IEEE Commun. Lett.*, vol. 18, no. 07, pp. 1218–1221, July 2014.

[29] T. Chakraborty, I. S. Misra, and T. Manna, "Design and implementation of VoIP based two-tier cognitive radio network for improved spectrum utilization," *IEEE Syst. J.*, vol. 10, no. 01, pp. 370–381, Mar. 2016.

[30] H.-J. Liu, Z.-X. Wang, S.-F. Li, and M. Yi, "Study on the performance of spectrum mobility in cognitive wireless network," in *Proc. ICCS*, 2008, pp. 1010–1015.

[31] H. Salameh, "Probabilistic spectrum assignment for QoS-constrained cognitive radios with parallel transmission capability," in *Proc. IFIP Wireless Days*, 2012, pp. 1–6.

[32] L.-C. Wang, C.-W. Wang, and C.-J. Chang, "Modeling and analysis for spectrum handoffs in cognitive radio networks," *IEEE Trans. Mobile Comput.*, vol. 11, no. 09, pp. 1499–1513, Sept. 2012.

[33] A. F. Tayel, S. I. Rabia, and Y. Abouelseoud, "An optimized hybrid approach for spectrum handoff in cognitive radio networks with non-identical channels," *IEEE Trans. Commun.*, vol. 64, no. 11, pp. 4487–4497, Nov. 2016.

[34] J. Wang, A. Huang, L. Cai, and W. Wang, "On the queue dynamics of multiuser multichannel cognitive radio networks," *IEEE Trans. Veh. Technol.*, vol. 62, no. 03, pp. 1314–1328, Mar. 2013.

[35] H. S. Hassanein and T. D. Todd, "Secondary VoIP capacity in opportunistic spectrum access networks with friendly scheduling," *IEEE Trans. Mobile Comput.*, vol. 15, no. 03, pp. 733–747, Mar. 2016.

[36] A. Alshamrani, X. Shen, and L.-L. Xie, "QoS provisioning for heterogeneous services in cooperative cognitive radio networks," *IEEE J. Sel. Areas Commun.*, vol. 29, no. 04, pp. 819–830, Apr. 2011.

[37] W. Gabran, C.-H. Liu, P. Paweczak, and D. Cabric, "Primary user traffic estimation for dynamic spectrum access," *IEEE J. Sel. Areas Commun.*, vol. 31, no. 03, pp. 544–558, Mar. 2013.

[38] Y. Saleem and M. H. Rehmani, "Primary radio user activity models for cognitive radio networks: A survey," *J. of Net. Compt. App.*, vol. 43, pp. 1–16, Apr. 2014.

[39] X. Li, X. Mao, D. Wang, J. McNair, and J. Chen, "Primary user behavior estimation with adaptive length of the sample sequence," in *Proc. Globecomm*, 2012, pp. 1308–1313.

[40] Q. Liu, S. Zhou, and G. B. Giannakis, "Cross-layer combining of adaptive modulation and coding with truncated ARQ over wireless links," *IEEE Trans. Wireless Commun.*, vol. 01, no. 07, pp. 1746–1755, Sept. 2004.

[41] Q. Liu, S. Zhou, and G. B. Giannakis, "Queuing with adaptive modulation and coding over wireless links: Cross-layer analysis and design," *IEEE Trans. Wireless Commun.*, vol. 04, no. 03, pp. 1142–1143, May 2005.

[42] C. Stevenson, G. Chouinard, Z. Lei, W. Hu, S. Shellhammer, and W. Caldwell, "IEEE 802.22: The first cognitive radio wireless regional area network standard," *IEEE Commun. Mag.*, vol. 01, no. 47, pp. 130–138, Jan. 2009.

[43] W.-Y. Lee, K. R. Chowdhury, and M. C. Vuran, "Spectrum sensing algorithms for cognitive radio networks," in *Cognitive Radio Networks*, 1st ed., Y. Xiao and F. Hu, Eds. Boca Raton, FL: CRC Press, 2009, pp. 4–34.

[44] C. Cordeiro, K. Challapali, D. Birru, and S. Shankar, "IEEE 802.22: An introduction to the first wireless standard based on cognitive radios," *Journal of Commun.*, vol. 01, no. 01, pp. 38–47, Apr. 2006.

[45] S. Buhari and F. Alagöz, "Scheduling in centralized cognitive radio networks for energy efficiency," *IEEE Trans. Veh. Technol.*, vol. 62, no. 02, pp. 582–595, Feb. 2013.

[46] V. K. Tumuluru, P. Wang, and D. Niyato, "A novel spectrum-scheduling scheme for multichannel cognitive radio network and performance analysis," *IEEE Trans. Veh. Technol.*, vol. 04, no. 60, pp. 1849–1858, May 2011.

Vita

Omar Khalid Sweileh was born in 1992, in Sharjah, in the United Arab Emirate. He was educated in local public schools and graduated from American University of Shariah with a double degrees in B.Sc. in computer engineering and B.Sc. in electrical engineering in Spring 2014. He was awarded the graduate teaching assistantship from the American University of Sharjah (AUS) and joined the Electrical Engineering Masters program in 2014. During his Masters degree, Mr. Sweileh also worked as a technical marketing engineer for one year at Intel Corp. in Dubai.